

PHILLIPS PETROLEUM COMPANY  
AUG 4 1947  
RESEARCH LIBRARY

15

# NATIONAL ADVISORY COMMITTEE FOR AERONAUTICS

TECHNICAL NOTE

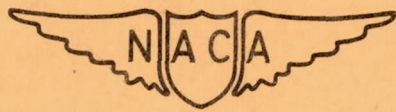
No. 1312

RECEIVED  
RESEARCH DEPT.  
AUG 4 1947  
CCB 8-4-47  
Lib

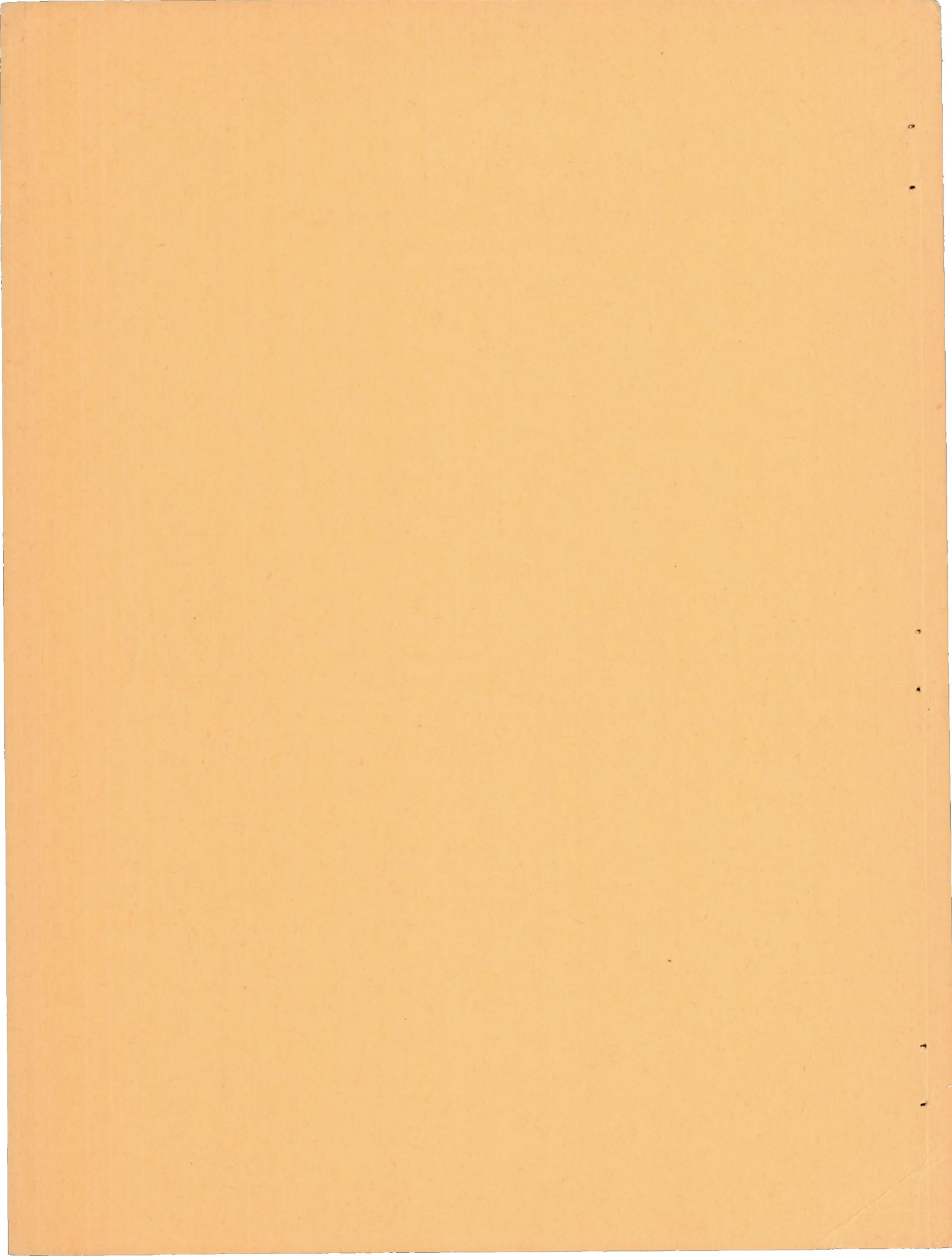
A COMPARATIVE STUDY OF WEIGHTS AND SIZES OF  
FLAT-PLATE EXHAUST-GAS-TO-AIR HEAT EXCHANGERS  
WITH AND WITHOUT FINS

By Thorval Tendeland and Charles P. Steinmetz

Ames Aeronautical Laboratory  
Moffett Field, Calif.



Washington  
July 1947



NATIONAL ADVISORY COMMITTEE FOR AERONAUTICS

---

TECHNICAL NOTE NO. 1312

---

A COMPARATIVE STUDY OF WEIGHTS AND SIZES OF  
FLAT-PLATE EXHAUST-GAS-TO-AIR HEAT  
EXCHANGERS WITH AND WITHOUT FINS

By Thorval Tendeland and  
Charles P. Steinmetz

SUMMARY

Analytical comparisons of weights and volumes are made for flat-plate heat exchangers having the same calculated thermal output and friction pressure drop for three different fin configurations; namely, (1) no fins, (2) fins in both the air and the exhaust gas passages, and (3) fins in the air passages only. Test data from two heat exchangers, one of configuration (1) and the other of configuration (2) are compared with the predicted weights and volumes. The thermal output and pressure-drop performance for these two exchangers, as evaluated from flight and ground tests, are also presented.

With the use of fins in both the air and the exhaust-gas passages, reductions in volume of the heat-exchanger core of significant magnitude can be obtained. Weight reductions with this fin arrangement depend upon the design fin efficiency and the thickness of the fluid passage gaps. The largest reductions in weight were obtained with the lowest design fin efficiencies investigated, namely 70 percent, and in exchangers which have a large number of passages with the same size air and exhaust-gas passage gaps. Reductions in weight and volume with fins in the air passages only are not so large as occur with the use of fins in both passages.

## INTRODUCTION

The performance of several exhaust-gas-to-air heat exchangers has been evaluated by ground tests made at the University of California (references 1 through 4) and by flight tests conducted at the Ames Aeronautical Laboratory (references 5 and 6). As a result of these tests, the practicability of various designs of heat exchangers as a source of heated air for a thermal ice-prevention system has been established; also important theoretical relationships for predicting the performances of various types of heat exchangers have been determined. The purpose of the current study is to investigate the possibility of reducing the over-all size and weight of flat-plate-type heat exchangers by the addition of fins to the surfaces. The flat-plate-type heat exchanger was selected for investigation because it possessed advantages, in relation to other types, in size and weight for specified values of heat-transfer rate and pressure drop.

The investigation was conducted in two parts: theoretical and experimental. Two representative heat exchangers were constructed and tested to verify the results of the analysis. Both the theoretical and experimental investigations were conducted at Ames Aeronautical Laboratory, Moffett Field, California.

## SYMBOLS

The symbols used throughout the report are as follows:

- A cross-sectional free-flow area of heat-exchanger core, square feet
- b fluid passage width, feet
- $c_p$  specific heat of fluid, Btu per pound, degree Fahrenheit
- $D_e$  equivalent or hydraulic diameter  $\left( \frac{4A}{L_p} \right)$ , feet
- d fluid passage gap, feet
- f friction factor for fluid flow, dimensionless

- G weight rate of fluid flow per unit cross-sectional area  
( $W/A$ ), pounds per hour, square foot
- h surface heat-transfer coefficient, Btu per hour, square foot,  
degree Fahrenheit
- k thermal conductivity, Btu per hour, square foot, degree  
Fahrenheit per foot
- K constant or factor, dimensionless
- L fluid passage length, feet
- $L_p$  wetted perimeter of fluid passage, feet
- $l_n$  no-flow dimension, feet
- N number of passages for one fluid
- $P_S$  static pressure, pounds per square foot
- $P_T$  total pressure, pounds per square foot
- $\Delta p$  pressure difference, pounds per square foot
- q dynamic pressure or velocity head, pounds per square foot
- Q rate of heat flow, heat output or enthalpy change, Btu per  
hour
- $R_o$  Reynolds number ( $D_o G/\mu$ ), dimensionless
- S heat-transfer-surface area, square feet
- t static temperature, degrees Fahrenheit
- $\Delta t$  static temperature difference, degrees Fahrenheit
- T absolute temperature ( $t + 460$ ), degrees Fahrenheit absolute
- $U_p$  over-all heat-transfer coefficient based upon a unit primary  
heat-transfer-surface area, Btu per hour, square foot,  
degrees Fahrenheit

V	velocity, feet per second
$V_c$	volume of heat-exchanger core, cubic feet
W	weight rate of fluid flow, pounds per hour
$W_c$	weight of heat-exchanger core, pounds
$W_x$	weight of finned surfaces, pounds
w	fin length, feet
y	metal thickness, feet
$\eta$	fin efficiency, dimensionless
$\rho$	mass density, slugs per cubic foot
$\mu$	absolute viscosity, pounds per hour, foot
$\gamma$	specific weight of heat-exchanger material, pounds per cubic foot

#### Subscripts

a	air side
av	average conditions
c	core
cf	cross flow
e	base of natural logarithms
E	expansion
F	surface friction
g	gas side
in	inlet conditions
M	mean
o	NACA standard conditions

p	plate or wall surfaces
out	outlet conditions
x	finned surfaces
test	test conditions
1,2,3,4,5	refer to stations of the heat-exchanger installation as tested in flight

### THEORETICAL INVESTIGATION

In order to determine if reductions in the size and weight of flat-plate-type heat exchangers by the addition of fins are possible, general equations for the performance of such heat exchangers must be developed and expressed in terms of the primary variables. The solutions to these general equations should provide a series of charts from which the optimum heat-exchanger designs can be selected for certain fixed initial conditions. By developing such design charts for both finned and unfinned heat exchangers, the relative size and weight advantages of either can be determined for the same initial conditions.

### ANALYSIS

The important factor which determines the weight and volume of an unfinned heat exchanger is the primary heat-transfer-surface area. Referring to figure 1, which is a sketch of the simplest type of flat-plate heat exchanger, it can be shown that the weight and volume of the core are

$$W_c = 2M_g b_a b_g \gamma_p \quad (1)$$

and

$$V_c = b_a b_g l_n$$

The weight of the core as expressed by equation (1) is that of the total flat-plate surface area, with the weight of structural members, flanges, welding material, etc., neglected.

A comparison of equations (1) and (2) indicates that the product  $b_a b_g$ , which is the area of one of the plates, is common to both equations. By expressing the heat-transfer-surface area as

$$S = 2 N_a b_a b_g \quad (3)$$

then the product  $b_a b_g$  is

$$b_a b_g = (S/2N_a) \quad (4)$$

Substituting the above value of  $b_a b_g$ , equations (1) and (2) become

$$W_c = (N_g/N_a) S y_p \gamma_p \quad (5)$$

and

$$V_c = (S l_n / 2N_a) \quad (6)$$

From equations (5) and (6) it is apparent that both core weight and volume vary directly with the heat-transfer-surface area. Thus for the same fluid passage gaps and number of passages, and the same plate metal material and thickness, both the weight and the volume of a flat-plate heat-exchanger core can be decreased by reducing the primary heat-transfer-surface area.

One method which seems likely to reduce the primary heat-transfer surface area is to utilize finned surfaces in both the



air and the exhaust-gas passages or in either of the passages. To obtain an indication of the practicability of the use of finned surfaces to reduce the primary heat-transfer-surface area, it is necessary to examine their effects upon the thermal output of the heat exchanger.

The total heat-transfer rate between the exhaust gas and air is

$$Q = U_p S \Delta t_M \quad (7)$$

where the over-all heat-transfer coefficient  $U_p$  is based upon a unit primary heat-transfer-surface area, and the mean temperature difference  $\Delta t_M$  (from reference 7) is

$$\Delta t_M = K_{cf} \frac{(t_{g_{in}} - t_{a_{in}}) - (t_{g_{out}} - t_{a_{out}})}{\log_e \left[ \frac{(t_{g_{in}} - t_{a_{in}})}{(t_{g_{out}} - t_{a_{out}})} \right]} \quad (8)$$

In equation (8), the factor  $K_{cf}$  is used to express the variation of the mean temperature difference between cross flow and parallel flow.

For given design conditions of thermal output, air and exhaust-gas flow rates, and inlet-air and exhaust-gas temperatures, the mean temperature difference in equation (7) is constant. Thus for the same thermal output, any increase in  $U_p$ , in equation (7), will result in a proportional decrease in  $S$ , the primary heat-transfer-surface area.

For an unfinned or all-primary heat-transfer-surface-type heat exchanger, the over-all heat-transfer coefficient as noted in reference 7 and neglecting the thermal resistance of the walls, is

$$U_p = \frac{1}{(1/h_g) + (1/h_a)} \quad (9)$$

where

$$h = 0.02 (k/D_e) (Re)^{0.8} \quad (10)$$

Equation (10) is applicable for turbulent flow of gases in round tubes and has been proven satisfactory for turbulent flow through rectangular channels when an equivalent or hydraulic diameter is used. With the addition of finned surfaces to both the air and the exhaust-gas passages, the expression for the over-all heat-transfer coefficient becomes

$$U_p = \frac{1}{\frac{1}{h_g \left\{ 1 + [(\eta S_x)_g/S] \right\}} + \frac{1}{h_a \left\{ 1 + [(\eta S_x)_a/S] \right\}}} \quad (11)$$

The effects upon  $U_p$  of the addition of fins to both the air and the exhaust-gas passages may be illustrated by assuming approximate values for the variables in equations (9) and (11). For example, assuming a ratio of effective fin area to primary surface area equal to 1 or  $(\eta S_x/S) = 1$ , and assuming equivalent values for the surface heat-transfer coefficients in both equations, the increase in  $U_p$  is 100 percent. Thus for the same thermal output, a reduction of the primary heat-transfer-surface area of 50 percent is possible.

The other fin arrangement considered is the addition of fins to either the air or the exhaust-gas passages. With fins in the air passages, the over-all heat-transfer coefficient is

$$U_p = \frac{1}{\frac{1}{h_g} + \frac{1}{h_a \left\{ 1 + [(\eta S_x)_a/S] \right\}}} \quad (12)$$

and with fins in the exhaust-gas passages,

$$U_p = \frac{1}{\frac{1}{h_g \left\{ 1 + [(\eta S_x)_g/S] \right\}} + \frac{1}{h_a}} \quad (13)$$

The increase in  $U_p$  with this fin arrangement can also be shown by assuming approximate values for the variables in equations (9), (12), and (13). Assuming  $h_a$  and  $h_g$  in all three equations equal to 20 and assuming  $(\eta S_x/S) = 1$  in equations (12) and (13), the

increase in  $U_p$  resulting from the addition of fins to one set of fluid passages is 34 percent. Therefore, it is apparent that for the same effective fin area the larger decrease in the primary heat-transfer-surface area can be obtained by using fins in both the air and the exhaust-gas passages. Because the heat-transfer coefficients,  $h_a$  and  $h_g$ , are of approximately the same magnitude in an exhaust-gas-to-air heat exchanger, the effective fin area should be made to be of the same magnitude for both the air and the exhaust-gas sides. For any value of effective fin area  $\eta S_x$ ,

equality of the terms  $h_a \left\{ 1 + [(\eta S_x)_a/S] \right\}$  and  $h_g \left\{ 1 + [(\eta S_x)_g/S] \right\}$  will result in the largest possible increase in the over-all heat-transfer coefficient  $U_p$ .

As may be noted from equation (3), the total primary heat-transfer-surface area can be reduced by decreasing either  $b_a$ ,  $b_g$ , or  $N_g$ . With the use of fins and for equivalent fluid passage gaps, decreasing either  $b_a$ ,  $b_g$ , or  $N_g$  results in an increase of the friction pressure drop of the heat-exchanger core when the fluid flow rates are constant. This increase in friction pressure drop is due to two causes; namely, (1) increasing the velocity of the air or exhaust gas in the heat-exchanger core as a result of decreasing the cross-sectional area for flow by decreasing either  $b_a$ ,  $b_g$ , or  $N_g$ , and (2) increasing the wetted surface perimeter by adding finned surfaces and thereby decreasing the hydraulic diameter of the fluid passages. The friction pressure drop for fluid flow in rectangular passages may be expressed, when an equivalent or hydraulic diameter is used, as follows:

$$\Delta P_F = f \frac{1}{2} \rho_{av} V_{av}^2 (4L/D_e) \quad (14)$$

To compensate for the increase in friction pressure drop resulting from the addition of fins, it is necessary to increase the gas-passage gaps, thereby increasing the no-flow dimension,  $l_n$ . As indicated by equation (2), an increase in the no-flow dimension may also increase the volume of the heat-exchanger core, depending

upon the magnitude of the decrease in  $b_a$  or  $b_g$  or both. Therefore, it appears probable that there will be an optimum gas passage gap at which the total core volume will be a minimum. The subsequent analysis was made in order to determine this point of minimum core weight and volume.

Families of heat exchangers of the following configurations were designed: (1) unfinned flat plate, (2) flat plate with fins in both the air and the exhaust-gas passages (3) flat plate with fins in the air passages only. The weights and volumes of the finned and unfinned units were then compared. The design conditions were the same for all three heat-exchanger configurations and are listed as follows:

	<u>Air Side</u>	<u>Gas Side</u>
Heat output, Btu/hr	250,000	250,000
Friction pressure drop, lb/sq ft	7.5	10
Flow rate, lb/hr	3500	3500
Inlet temperature, °F	59	1600
Inlet pressures, lb/sq in.	14.7	14.7

The design of the heat exchangers was accomplished by expressing the relationship for over-all heat-transfer rate (equation (7)) and the relationships for friction pressure drop for both air and exhaust gas (equation (14)) in terms of the fluid-passage dimensions  $b$  and  $d$  and the number of passages  $N$ . These relationships were then solved simultaneously for expressions for the fluid-passage dimensions in terms of the following variables:

1. Number of air and exhaust-gas passages  $N_a$ ,  $N_g$
2. Specific properties of the gases  $k_a$ ,  $k_g$ ,  $\mu_a$ ,  $\mu_g$ ,  $\rho_a$ ,  $\rho_g$
3. Weight-flow rates  $W_a$ ,  $W_g$
4. Friction pressure drops  $(\Delta p_F)_a$ ,  $(\Delta p_F)_g$
5. Heat output  $Q$
6. Mean temperature difference  $\Delta t_M$

The fluid passage dimensions  $b_a$ ,  $b_g$ , and  $d_g$  were then determined by assuming the number of air passages  $N_a$  and the air passage gap  $d_a$ . Simplification of the equations, which apply with the use of finned surfaces, was effected by the following assumptions:

1. The reduction in free cross-sectional area for flow in a gas passage was negligible due to the presence of the fins.
2. The ratio of flat-plate or wall surface area to fin area was 0.707.

The second assumption results from arranging the fins in the form of triangular corrugations in the gas passages, with each side of a corrugation at an angle of  $45^\circ$  to the wall surfaces.

The weight of the finned surfaces in the air passages and for the fins in the exhaust-gas passages was computed as follows:

$$W_x = \frac{N_a b_a b_g \gamma_x \gamma_x}{\cos 45^\circ} \quad (15)$$

$$W_x = \frac{N_g b_a b_g \gamma_x \gamma_x}{\cos 45^\circ} \quad (16)$$

The specific weight of the fins  $\gamma_x$  used in equations (15) and (16) was that of stainless steel.

The thickness of the fins was determined from the design fin efficiency and the gas-passage gap. The expression for fin efficiency, as given in reference 8, is

$$\eta = \frac{\tanh aw}{aw} \quad (17)$$

where

$$a = \sqrt{2h/k_x \gamma_x}$$

As may be noted from equation (17), the variables in the geometric design of the fins which determine their efficiency are the fin length and thickness. The arrangement of the fins in a fluid passage established their length as

$$w = \frac{d}{2 \cos 45^\circ} \quad (18)$$

Thus by means of equations (17) and (18) and the design fin efficiencies, the thickness of the fins was computed. In equation (17) an average heat-transfer coefficient of 20 Btu per hour, square foot,  $^\circ\text{F}$  and the thermal conductivity of stainless steel based upon a temperature of  $900^\circ\text{F}$  were assumed. These assumptions were found to be representative of calculated heat-transfer coefficients and wall temperatures for several of the heat exchangers designed. The thermal conductivity of stainless steel obtained from reference 9 for a temperature of  $900^\circ\text{F}$  was 12.2 Btu per hour, square foot,  $^\circ\text{F}$  per foot. The range of fin thicknesses for the fin efficiencies and fluid passage gaps investigated is specified as follows:

1. For a fin efficiency of 70 percent, the fin thickness was 0.004 inch for a 0.2-inch gap, and 0.025 inch of a 0.5-inch gap.
2. For a fin efficiency of 90 percent, the fin thickness was 0.015 inch for a 0.2-inch gap, and 0.10 inch for a 0.5-inch gap.

The weight of the flat-plate surface area was determined by means of equation (1). The plate material was assumed to be 0.032-inch-thick stainless steel. This metal thickness was chosen as approximately the minimum required for satisfactory service life and was based on past experience in flat-plate heat-exchanger construction (reference 5). The volumes of the heat-exchanger cores were determined by means of equation (2).

#### RESULTS OF ANALYSIS

Design charts which show the dimensions of the fluid passages for the finned and unfinned heat exchangers are shown in figure 2. The dimensions of the fluid passages were determined by means of equations (7) and (14). In these charts the passage dimensions  $b_a$ ,  $b_g$ , and  $d_g$  are plotted as a function of the air-passage gap  $d_a$  with the number of air passages as a parameter. These charts were used to calculate the weights and volumes of the heat-exchanger cores. It is apparent from figure 2 that, for a given air gap and number of passages, a large reduction in  $b_g$  and a small increase in  $b_a$  result from the addition of finned surfaces, thus indicating a considerable reduction in the primary heat-transfer-surface area. However, an increase of the no-flow dimension for

the finned heat exchangers is indicated by the larger gaps of the exhaust-gas passages.

Figure 3 shows a comparison of volumes between the heat exchangers without fins and with fins in both the air and the exhaust-gas passages. In this figure the volumes of the heat-exchanger cores have been plotted as a function of the air-passage gap. To indicate possible trends, comparisons were made for families of heat exchangers with 10, 15, 20, and 30 air passages and for heat exchangers with fin efficiencies of 70, 80, and 90 percent. Inspection of the curves indicates that, for both the finned and the unfinned heat exchangers, increasing the number of air passages  $N_a$  greatly decreases the core volume; also for a given number of passages, a considerable saving in the over-all size or volume is possible by the use of fins. As would be expected the smallest heat exchangers are those with the most efficient fins. It is also noticeable that the addition of fins increases the optimum air-gap thickness and that as the number of passages increases the optimum air-gap thickness decreases for both the finned and the unfinned heat exchangers. From figures 2 and 3 it may be seen that the minimum volume of the finned and unfinned heat exchangers occurs when the air and exhaust-gas passage gaps for each type of exchanger are the same.

Figure 4 shows comparisons between the weights of the heat exchangers without fins and with fins in both the air and the exhaust-gas passages. It is apparent from this figure that, with a small number of fluid passages and with 90-percent efficient fins, increases in the weight of the core results with the use of fins. With a small number of fluid passages, as indicated in figure 2, the exhaust-gas passage gaps are large as compared to the exhaust-gas passage gaps when there are a large number of passages. Therefore, for high fin efficiencies, thicker fins must be used in the exhaust-gas passages, thereby increasing the weight of the core. With less efficient fins and particularly with a large number of passages, the use of fins results in a reduction in weight, with the maximum reduction in weight occurring when the air and the exhaust-gas passages are of the same thickness.

It is of interest to note that for the finned heat exchangers the minimum weight and volume occurs for the same air-passage gap for a given number of passages. However, for a thermal ice-prevention system, the heat exchanger is usually selected with dimensions which will meet the space requirements. These dimensions may not correspond to those of minimum weight and volume.

For all practical purposes, the weights of the unfinned heat exchangers are essentially constant as the air-passage gap is varied. Reductions in weight are achieved for the unfinned heat exchangers by increasing the number of passages. However, with an increase in the number of passages the weight reduction is not as large as compared with the finned units.

Figures 5 and 6 are comparisons of volume and weight, respectively, between families of unfinned exchangers and exchangers with fins in the air passages only. These figures indicate reductions in the volume are possible by using fins in the air passages only, but the magnitude of the reductions is not as large as with fins in both the air and the exhaust-gas-passages. Weight reductions are obtainable with small air-passage gaps where design fin efficiencies can be obtained by using short thin fins which are light. For low fin efficiencies and with a large number of gas passages, the reduction in weight when using fins in the air passages only is not as large as with the addition of fins to both the air and the exhaust-gas passages.

#### EXPERIMENTAL INVESTIGATION

To check the design procedure used in the analysis and to obtain comparisons with the predicted weights and volumes, a finned and unfinned heat exchanger were built and tested. A description of these two heat exchangers and the experimental technique used to evaluate their performances are presented herein.

#### DESCRIPTION OF EQUIPMENT AND INSTRUMENTATION

The design features of the finned and unfinned heat exchangers were similar. Details of the two heat-exchanger cores are shown in figures 7 through 10. Previous experience with flat-plate heat-exchanger construction has indicated that the plate material should be either stabilized stainless steel or Inconel. For the plain plate heat exchanger, the plates were formed from 0.032-inch-thick Inconel. Spacers were placed in both the air and the exhaust-gas passages of this unit to prevent the plates from warping and buckling due to the high temperatures encountered.



For the finned heat exchanger, the fins were shaped in the form of corrugations or equally spaced ridges. The fin material was 0.015- and 0.032-inch-thick stainless steel for the air and the exhaust-gas fins, respectively. The plates were formed from 0.032-inch-thick stainless steel. The fins or corrugated sheets were placed within the gas passages and attached to the plates at the tops and bottoms of the corrugations. With this arrangement each side of a single corrugation formed two fins; also the fins acted as spacers and stiffeners, thus preventing the plates from warping. Before assembling the core of the heat exchanger, the plates and fins were thoroughly cleaned and then coated with a thin layer of copper by a spraying process. When assembled the core was jugged and brazed in a controlled-atmosphere furnace. During the furnace-brazing process some warpage of the plates in the outside air and the exhaust-gas passages occurred, resulting in poor bonds between the fins and plates in these passages. Retouching of some of the plate joints was done by flame brazing.

The heat exchangers were flight-tested on a three-place observation-type airplane powered by a radial engine rated at 835 horsepower at 3900 feet altitude. A more complete description of the airplane is given in reference 6. The unfinned heat exchanger when installed for flight tests is shown in figure 11.

The shrouding or headers employed in the flight tests consisted of transitions between the round exhaust stack and ducting, and the rectangular contours of the heat exchangers. The headers used in the determination of core pressure drop in ground tests consisted of straight rectangular ducting, free from any pressure losses other than that due to skin friction.

The instrumentation used in flight-testing the unfinned heat exchanger and the location of the instrumentation in the test installation are shown in figure 12. For the flight tests of the finned heat exchanger, the instrumentation differed from that shown in figure 12 in that the pressure-survey rakes and the static wall orifices in the exhaust stack were not used. In these tests the nonisothermal pressure drop of the heat exchanger was not measured. For the tests of both heat exchangers, air and exhaust-gas flow rates were measured with venturi meters located downstream from the heat exchanger. Air temperatures were measured with two bare iron-constantan thermocouples upstream from the heat exchanger and six downstream, all equally spaced across the ducting diameter. Exhaust-gas temperatures were measured with quadruple-shielded thermocouples, one located upstream and one downstream from the

heat exchanger. The shielded thermocouples were located at the center of the exhaust stack.

For the flight tests of the unfinned heat exchanger, the total-pressure drop across the heat exchanger on the air side was measured with two pressure survey rakes. (See fig. 13.) On the exhaust-gas side, the static-pressure drop was measured by means of three static-wall orifices upstream and four static tubes downstream from the heat exchanger. The four static tubes were a part of a pressure-survey rake (fig. 13) used to check the exhaust-gas-flow rates as determined from the venturi meter.

#### TEST PROCEDURE

Flight testing of the heat exchangers was conducted to evaluate their thermal performances and to determine the nonisothermal pressure drop of the unfinned heat-exchanger core. Ground tests were made to determine the isothermal core pressure drops and also the isothermal pressure drop of the headers used in flight-testing the unfinned exchanger.

#### Flight Tests

Flight testing of the heat exchangers was conducted in level flight at 5,000 and 15,000 feet pressure altitudes. The exhaust-gas-flow rates were regulated by adjusting the manifold pressure and engine speed to obtain desired weight flow rates of approximately 3200, 4200, and 5200 pounds per hour. However, due to the limited capacity of the engine at 15,000 feet pressure altitude, only the lowest flow rate of 3200 pounds per hour could be obtained. An inlet exhaust-gas temperature of approximately 1600° F was obtained by adjusting the fuel-air ratio. The air-flow rate was regulated by means of a valve in the outlet-air duct. For each exhaust-gas flow rate, measurements were taken at the maximum air-flow rate obtainable and at several reduced air-flow rates.

#### Ground Tests

Ground tests of the unfinned heat exchanger were made to determine the components of the isothermal pressure drop across the heat-exchanger installation as tested in flight. This was accomplished by testing the heat-exchanger core, both air and exhaust-gas sides, when equipped with the following combinations of headers:

1. Inlet and outlet straight headers
2. Inlet straight header and outlet flight header
3. Inlet flight header and outlet straight header

During each test, air at room temperature was drawn through the heat exchanger at flow rates varying from 1000 to 6000 pounds per hour. Static pressures upstream and downstream from the heat-exchanger core were measured with static tubes, and air flow rates were measured with a venturi meter. All measured static-pressure drops were corrected for area differences in those tests in which the measurements were made in ducting of unequal cross-sectional area. The pressure drop of the heat-exchanger core was obtained when the heat exchanger was tested with both straight headers, since the component of pressure drop contributed by the straight headers was calculated and found to be negligible. The pressure drop of a flight header was determined by subtracting the pressure drop of the core from the measured pressure drop of the heat exchanger when equipped with a single flight header. As a check of the sum of the component pressure drops, the heat exchanger was tested when equipped with both flight headers. Ground tests of the finned heat exchanger consisted of measuring the pressure drop of the core when equipped with straight inlet and outlet headers on the air and the exhaust-gas sides.

#### PRECISION OF MEASUREMENTS

The venturi meters used to measure the exhaust-gas and the air flow rates were calibrated against a sharp-edged orifice. A comparison of flow rates as measured by the venturi meters and pressure-survey rakes indicated agreement within  $\pm 6$  and  $\pm 5$  percent for the exhaust-gas and air flow rates, respectively.

The inlet-air temperature was measured by means of two bare iron-constantan thermocouples which indicated temperatures within  $2^{\circ}$  F and  $3^{\circ}$  F of the standard free-air temperature installation.

The outlet-air temperature was taken as the arithmetical average of the temperatures as indicated by the six bare iron-constantan thermocouples. Radiation errors in the thermocouple readings were reduced by lagging the ducting with 1/4-inch asbestos. It is estimated the maximum error in determining the average outlet-air temperature

was  $\pm 10^{\circ}$  F. The exhaust-gas temperatures were measured at the center of the exhaust stack. Radiation errors were minimized by using quadruple-shielded thermocouples and by lagging the exhaust stack with 1/4-inch asbestos. It is estimated the maximum error in determining the average exhaust-gas temperature was  $\pm 40^{\circ}$  F. The measured air and exhaust-gas temperatures were not corrected for adiabatic temperature rises, since the velocities at the points of measurement were not large.

For the flight tests, the average total pressure at a station on the air side was the arithmetical mean of the total-pressure measurements. Since the multicell manometers used to record pressure measurements were calibrated, the error in the use of the instruments was principally that of reading the film records. It is estimated that the maximum error in the nonisothermal pressure-drop measurements was  $\pm 1.5$  pounds per square foot. For the ground tests, micromanometers were used in the pressure measurements. It is believed the error in the isothermal pressure-drop measurements was small.

Based upon consideration of the accuracy of measurements, it is estimated the maximum error in determining the thermal outputs of the heat exchangers was  $\pm 8$  percent.

#### EXPERIMENTAL RESULTS

The volumes and weights of the finned and the unfinned heat exchangers, which were built and tested, are shown in figures 3(c) and 4(c), respectively. The thermal performances of the two exchangers as evaluated from the air-side enthalpy change together with the predicted thermal output of the unfinned heat exchanger are shown in figure 14. The thermal outputs of the two heat exchangers as evaluated from test data were corrected to equivalent initial temperature conditions by the method given in the appendix. Nonisothermal pressure-drop data for the unfinned heat exchanger as measured in flight and when reduced to NACA standard conditions of temperature and pressure are shown in figures 15 and 16. Predicted isothermal pressure drops and test data for both heat exchangers are compared at standard conditions in figure 17. The method of reducing the pressure-drop data to standard conditions is given in the appendix.

## DISCUSSION

The volumes of the finned and the unfinned heat-exchanger cores as noted in figure 3(c) were calculated as the product of  $b_a$ ,  $b_g$ , and  $l_n$ . These volumes were used in preference to those determined from the measured over-all dimensions due to the effects of construction features upon the over-all dimensions. These features, namely, the protrusions of the flanges from the plates, are characteristic of this heat-exchanger design and have no particular effect upon the heat-transfer or pressure-drop performances.

From inspection of figure 3(c) it may be noted that the volume of the heat exchanger with finned surfaces is higher than the predicted value. In fabricating the fins, allowances for radii to bend the fins in the form of corrugations were necessary and, as a result, the ratio of fin area to primary heat-transfer-surface area was less than the design ratio of 1/0.707. To compensate for this reduction in fin area, the primary heat-transfer area was increased by increasing the dimensions  $b_a$  and  $b_g$ . This increase in  $b_a$  and  $b_g$  also compensated for the reduction in free cross-sectional area of the gas passages due to the presence of the fins. Thus, with an increase of two of the dimensions of the heat exchanger, the resulting volume was larger than predicted.

The weights of the cores of the finned and unfinned heat exchangers, as noted in figure 4(c), were 44-1/2 pounds and 49-1/2 pounds, respectively. The magnitude of the reduction in weight with the use of fins compares favorably with the predicted values of 26 and 30-1/2 pounds. However, this agreement may be fortuitous since the predictions are based only on the weight of the flat-plate-surface areas plus the weight of the fins for the finned unit. The weights of the completed cores included the additional weight of flanges, spacers, brazing material, etc.

To compare the thermal outputs at equivalent test conditions, all data were corrected to an initial air to exhaust-gas temperature difference of 1500° F. This temperature difference was chosen since it approximates the test conditions of this investigation and those encountered by a heat exchanger in a thermal ice-prevention system. Inspection of figure 14 shows good agreement between the thermal performances of the two heat exchangers. The thermal output of approximately 245,000 Btu per hour at air and exhaust-gas flow rates of 3500 and 3250 pounds per hour, respectively, compares favorably with the design output of 250,000 Btu per hour. The

design output was based upon an air and exhaust-gas flow rate of 3500 pounds per hour and an initial air-exhaust-gas-temperature difference of  $1541^{\circ}$  F.

The pressure-drop performances of the two heat exchangers were compared on the basis of the static-pressure drop across the heat-exchanger cores at temperature and pressure conditions which correspond to NACA standard sea-level atmosphere. In isothermal flow, static-pressure drop is approximately equivalent to total-pressure drop when measured at stations of equal area, if the velocity distribution across the two stations is postulated to be the same. The method of reducing the measured isothermal and nonisothermal pressure-drop data to standard conditions, as shown in the appendix, is substantiated by the data presented in figures 15 and 16.

The predicted isothermal pressure drops for both heat exchangers as shown in figure 17 include the friction pressure drops and the expansion pressure drops at the outlets of the cores. The entrance losses were assumed negligible, since the entry into the individual passages was smooth and well rounded. Inspection of figure 17 indicates that the predicted and experimental pressure drop for the finned heat exchanger are slightly lower than the corresponding pressure drops for the unfinned unit. This is due to the lower expansion pressure losses at the outlet of the fluid passages for the finned unit.

#### CONCLUSIONS

Based upon the comparative weights and volumes of families of finned and unfinned flat-plate-type heat exchangers, designed for equivalent heat-transfer and friction-pressure drop performances, it is concluded:

1. A considerable reduction in over-all size or volume results with the use of fins in both the air and the exhaust-gas passages. The largest reductions in volume occur with the use of fins with high efficiencies. For the two heat exchangers built, the volume of the finned unit was approximately 18 percent less than the unfinned unit.

2. The reduction in weight with the use of fins in both the air and the exhaust-gas passages depends upon the design efficiency of the fins and the dimensions of the fluid passage gaps. The

largest reductions in weight were obtained with the lowest design fin efficiencies investigated, namely 70 percent, and in exchangers which have a large number of passages with the same size air and exhaust-gas passage gaps. For a heat exchanger constructed with fins of 70-percent design efficiency, the reduction in weight compared to an unfinned unit was approximately 10 percent.

3. With fins in the air passages only, the reduction in volume is not as large as compared to units with fins in both the air and the exhaust-gas passages. Weight reductions with this fin arrangement are obtainable in units with small air-passage gaps.

Ames Aeronautical Laboratory,  
National Advisory Committee for Aeronautics,  
Moffett Field, Calif., April 21, 1947.

## APPENDIX

## REDUCTION OF DATA TO EQUIVALENT CONDITIONS OF TEMPERATURES AND PRESSURE

## Reduction of Thermal Data

The correction applied to the thermal outputs of the heat exchangers was determined from the over-all heat-transfer rate which, expressed in the notation used in this report, is

$$Q = U_p S \Delta t_M \quad (19)$$

or

$$Q = U_p S K_{cf} \frac{(t_{gin} - t_{ain}) - (t_{gout} - t_{aout})}{\log_e [(t_{gin} - t_{ain}) / (t_{gout} - t_{aout})]} \quad (20)$$

Determining  $t_{aout}$  and  $t_{gout}$  from enthalpy changes on the air and exhaust-gas sides

$$t_{aout} = (Q / W_a c_{pa}) + t_{ain}$$

and

$$t_{gout} = t_{gin} - (Q / W_g c_{pg})$$

With these values of  $t_{aout}$  and  $t_{gout}$ , equation (20), when reduced, then becomes

$$Q = (t_{gin} - t_{ain}) \left( \frac{W_g c_{pg} W_a c_{pa}}{W_a c_{pa} + W_g c_{pg}} \right) \left\{ 1 - \frac{1}{e^{U_p S K_{cf} [(1/W_g c_{pg}) + (1/W_a c_{pa})]}} \right\} \quad (21)$$

It may be noted from this expression that the thermal output at constant air and exhaust-gas flow rates is a function of  $t_{gin} - t_{ain}$ ,  $c_{pg}$ ,  $c_{pa}$ , and  $U_p$ . Because  $c_{pg}$ ,  $c_{pa}$ , and  $U_p$  vary



only slightly with temperature, the thermal output varies linearly with  $t_{gin} - t_{ain}$ . Hence, the correction to reduce the thermal output to standard inlet-temperature conditions is

$$Q_o = Q_{test} \left[ \frac{(t_{gin} - t_{ain})_o}{(t_{gin} - t_{ain})_{test}} \right] \quad (22)$$

#### Reduction of Isothermal Pressure-Drop Data

The isothermal pressure drop of the heat-exchanger core at standard NACA conditions of temperature and pressure may be expressed as

$$(\Delta p_c)_o = (\Delta p_F)_o + (\Delta p_E)_o \quad (23)$$

In equation (23) the heat-exchanger core-entrance loss was assumed negligible since the entry into the individual air and exhaust-gas passages was smooth and well rounded. Correlating  $(\Delta p_F)_o$  and  $(\Delta p_E)_o$  with the corresponding pressure drops at test conditions

$$(\Delta p_F)_o = (\Delta p_F)_{test} \left\{ \frac{[f q_c (4L/D_e)]_o}{[f q_c (4L/D_e)]_{test}} \right\} \quad (24)$$

and

$$(\Delta p_E)_o = (\Delta p_E)_{test} \left\{ \frac{[(1-K)^2 q_c]_o}{[(1-K)^2 q_c]_{test}} \right\} \quad (25)$$

where  $K$  in equation (25) is the ratio of the cross-sectional free area of the core to the area of the outlet header. With these values of  $(\Delta p_F)_o$  and  $(\Delta p_E)_o$  equation (23), when reduced, then becomes

$$(\Delta p_c)_o = (\Delta p_F) \left( \frac{\rho_{test}}{\rho_o} \right) \left( \frac{T_o}{T_{test}} \right)^{0.13} + (\Delta p_E) \left( \frac{\rho_{test}}{\rho_o} \right) \quad (26)$$

The temperature correction  $(T_0/T_{\text{test}})^{0.13}$  which applies to the friction pressure drop, corrects for changes in friction factor with Reynolds number. Neglecting this correction results in only a small error, since the isothermal tests were run at room temperature, and simplifies the reduction of isothermal pressure-drop data to merely a density correction, or

$$(\Delta p_c)_0 = (\Delta p_c)_{\text{test}} \left( \frac{\rho_{\text{test}}}{\rho_0} \right) \quad (27)$$

#### Reduction of Nonisothermal Pressure-Drop Data

Referring to the stations shown in figure 12, the air-side nonisothermal total pressure drop of the heat-exchanger core was determined from the measured total-pressure drop of the heat-exchanger installation as follows:

$$(\Delta p_c)_T = (\Delta p)_{1-6} - K_{\text{in}}(q_2) - K_{\text{out}}(q_3) - (\Delta p_f)_{5-6} \quad (28)$$

The inlet flight-header pressure drop  $K_{\text{in}}(q_2)$  and the outlet flight-header pressure drop  $K_{\text{out}}(q_3)$  were evaluated by means of ground tests. The coefficients  $K_{\text{in}}$  and  $K_{\text{out}}$  are the ratio of the flight-header pressure drop to the velocity head at the inlet and outlet of the heat-exchanger core, respectively. The friction pressure drop  $(\Delta p_f)_{5-6}$  in the ducting downstream from the heat exchanger was calculated.

From the nonisothermal total-pressure drop of the heat-exchanger core,

$$\Delta p_F + \Delta p_E = (\Delta p_c)_T - (q_3 - q_2) \quad (29)$$

where  $q_3 - q_2$  is the momentum pressure drop. In order to apply the proper corrections the magnitudes of  $\Delta p_F$  and  $\Delta p_E$  must be known. The proportional distribution of the sum  $\Delta p_F + \Delta p_E$  into its components was determined from the analytical predictions

of the nonisothermal pressure drop of the core. The total pressure drop of the core at NACA standard conditions of temperature and pressure is then

$$(\Delta p_c)_o = (\Delta p_F)' \left( \frac{\rho_{av}}{\rho_o} \right) \left( \frac{T_o}{T_{av}} \right)^{0.13} + (\Delta p_E)_o \left( \frac{\rho_3}{\rho_o} \right) \quad (30)$$

The method of evaluating and reducing the static-pressure drop of the heat-exchanger core on the exhaust-gas side was similar to that used on the air side. The differences in the two methods were (1) in determining the static-pressure drop of the core, corrections were necessary to adjust for area differences between the heat-exchanger core and the stations at which the measurements were taken; (2) the change in pressure due to a change in momentum on the exhaust-gas side was  $2(q_3 - q_2)$  as compared to  $q_3 - q_2$  on the air side.

In figures 15 and 16 are presented the nonisothermal pressure-drop data for the unfinned heat exchanger as measured in flight and when reduced to standard conditions of temperature and pressure. A comparison also is made in figure 16 between these data at standard conditions and the measured isothermal pressure drop. The agreement between these two sets of data is fair with some scatter on the air side at the lower air flow rates. However, the agreement does indicate the method of reducing the nonisothermal pressure-drop data is satisfactory. By eliminating the effects of temperature and pressure with various test conditions, this comparison illustrates that the basic pressure-drop measurement, to establish the pressure drop performance, is the isothermal total pressure drop across the heat-exchanger core. This conclusion is further substantiated after examining the components of the nonisothermal pressure drop, which, on the air side, may be expressed as

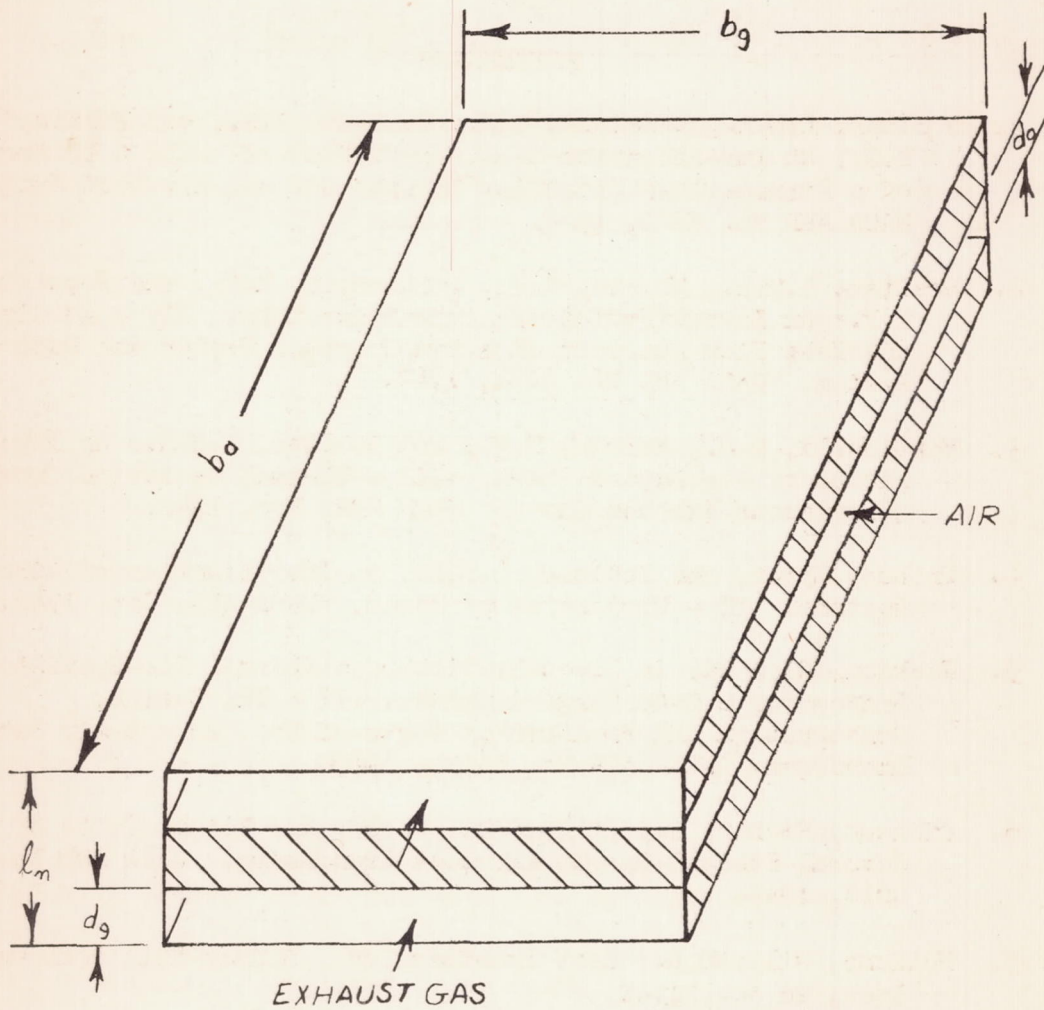
$$(\Delta p_c)_{test} = (\Delta p_F)_o \left( \frac{\rho_o}{\rho_{av}} \right) \left( \frac{T_{av}}{T_o} \right)^{0.13} + (\Delta p_E) \left( \frac{\rho_o}{\rho_3} \right) + (q_3 - q_2) \quad (31)$$

The change in pressure  $q_3 - q_2$  due to an increase in momentum of the fluid is not necessarily a totally irrecoverable pressure loss. This pressure drop may be partially recovered, depending upon the drop in temperature of the fluid in the system after the heat exchanger. On the exhaust-gas side, the change in pressure due to a decrease in momentum of the fluid results in a decrease in pressure drop. The density corrections which apply to  $(\Delta p_F)_o$  and  $(\Delta p_E)_o$

are those due to variations in temperature of the fluid through the core and changes in pressure with altitude. Isothermal total-pressure drop at standard conditions represents skin friction, expansion, contraction, or turning losses at a standard temperature and pressure, and are irrecoverable losses.

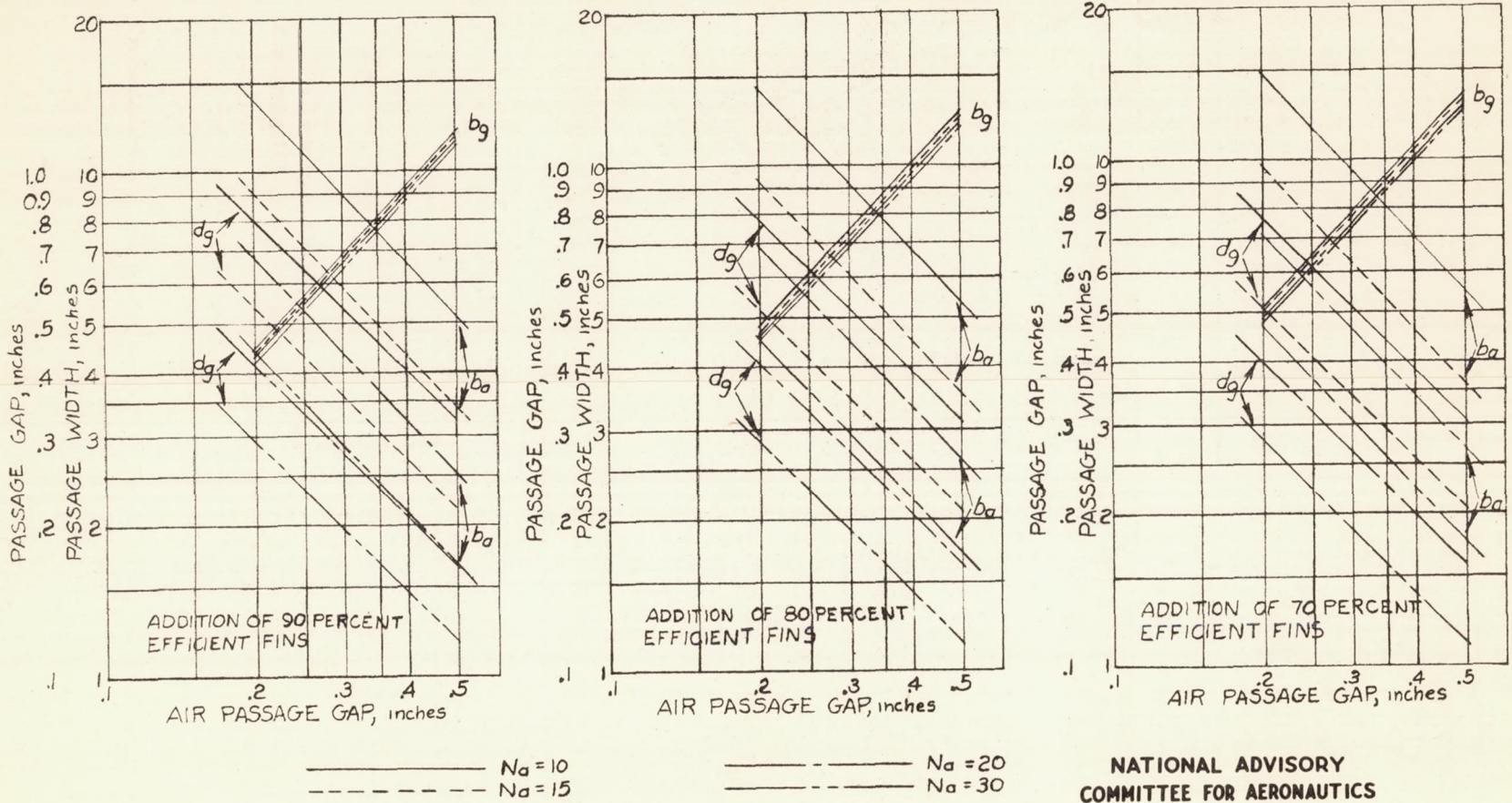
## REFERENCES

1. Boelter, L.M.K., Dennison, H.G., Guibert, A.G., and Morrin, E.H.: An Investigation of Aircraft Heaters. XII - Performance of a Formed-Plate Crossflow Exhaust Gas and Air Heat Exchanger. NACA ARR No. 3E10, 1943.
2. Boelter, L.M.K., Morrin, E.H., Martinelli, R.C., and Poppendick, H.F.: An Investigation of Aircraft Heaters. XIV - An Air and Heat Flow Analysis of a Ram-Operated Heater and Duct System. NACA ARR No. 4C01, 1944.
3. Martinelli, R.C., Morrin, E.H., and Boelter, L.M.K.: An Investigation of Aircraft Heaters. VII - Thermal Radiation from Athermanous Exhaust Gases. NACA ARR, Dec. 1942.
4. Tribus, Myron, and Boelter, L.M.K.: An Investigation of Aircraft Heaters. II - Properties of Gases. NACA ARR, Oct. 1942.
5. Jackson, Richard: An Investigation of a Thermal Ice-Prevention System for a C-46 Cargo Airplane. II - The Design, Construction and Preliminary Tests of the Exhaust-Air Heat Exchanger. NACA ARR No. 5A03a, 1945.
6. Jackson, Richard and Hillendahl, Wesley H.: Flight Tests of Several Exhaust-Gas-To-Air Heat Exchangers. NACA ARR No. 4C14, 1944.
7. McAdams, William H.: Heat Transmission. McGraw-Hill Book Co., Inc., 2d ed., 1942.
8. Harper 3d, D.R., and Brown, W.B.: Mathematical Equations for Heat Conduction in the Fins of Air-Cooled Engines. NACA Rep. No. 158, 1922.
9. Bernardo, Everett, and Eian, Carrol S.: Heat-Transfer Tests of Aqueous Ethylene Glycol Solutions in an Electrically Heated Tube. NACA ARR No. E5F07, 1945.



NATIONAL ADVISORY  
COMMITTEE FOR AERONAUTICS

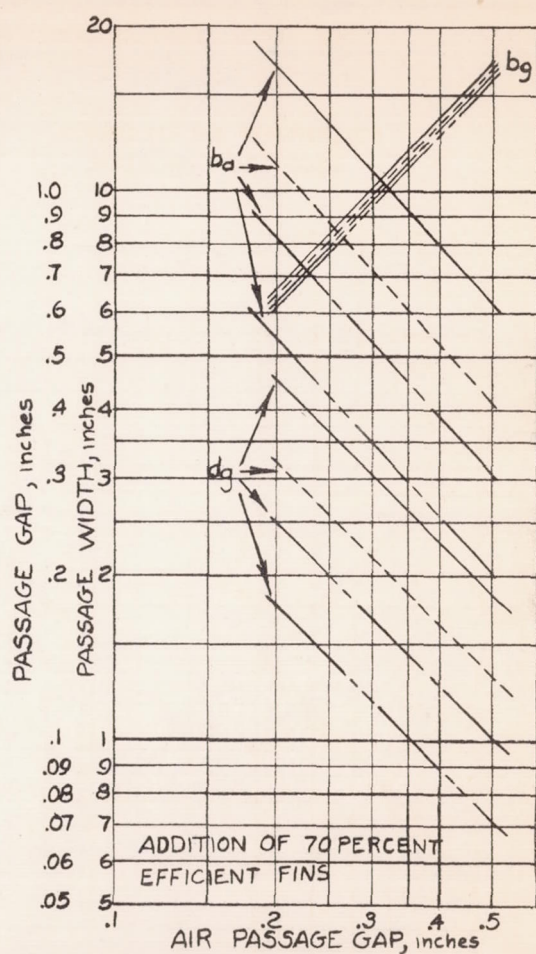
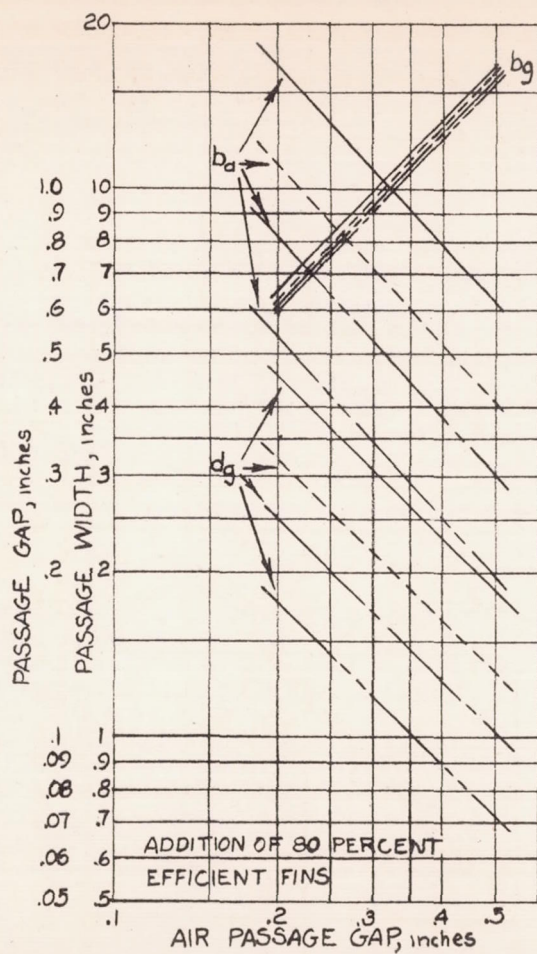
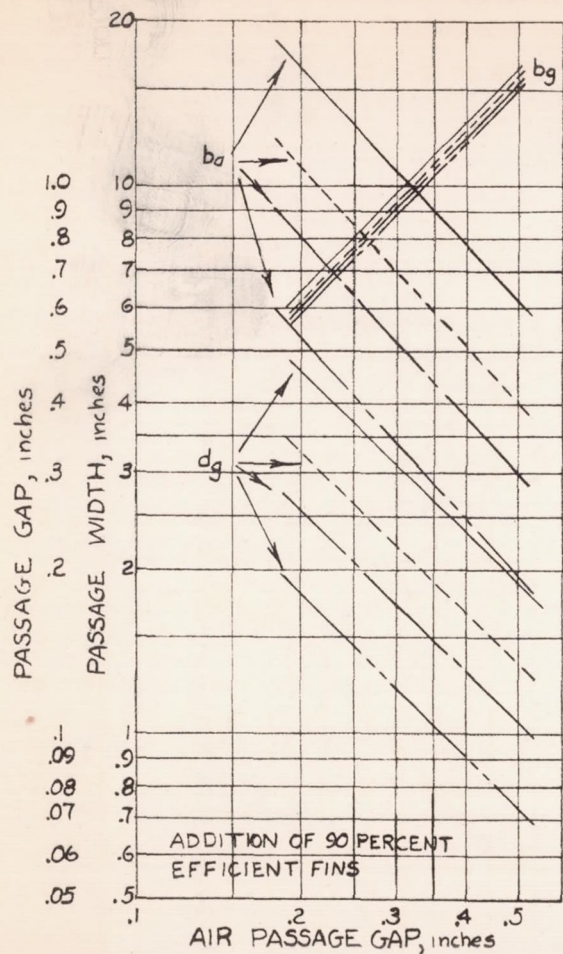
FIGURE 1.- SKETCH OF A FLAT-PLATE HEAT EXCHANGER.



(a) FINS IN BOTH AIR AND EXHAUST-GAS PASSAGES.

FIGURE 2.- VARIATION OF HEAT-EXCHANGER DIMENSIONS WITH AIR-PASSAGE GAP AND THE NUMBER OF AIR PASSAGES.

NATIONAL ADVISORY  
COMMITTEE FOR AERONAUTICS



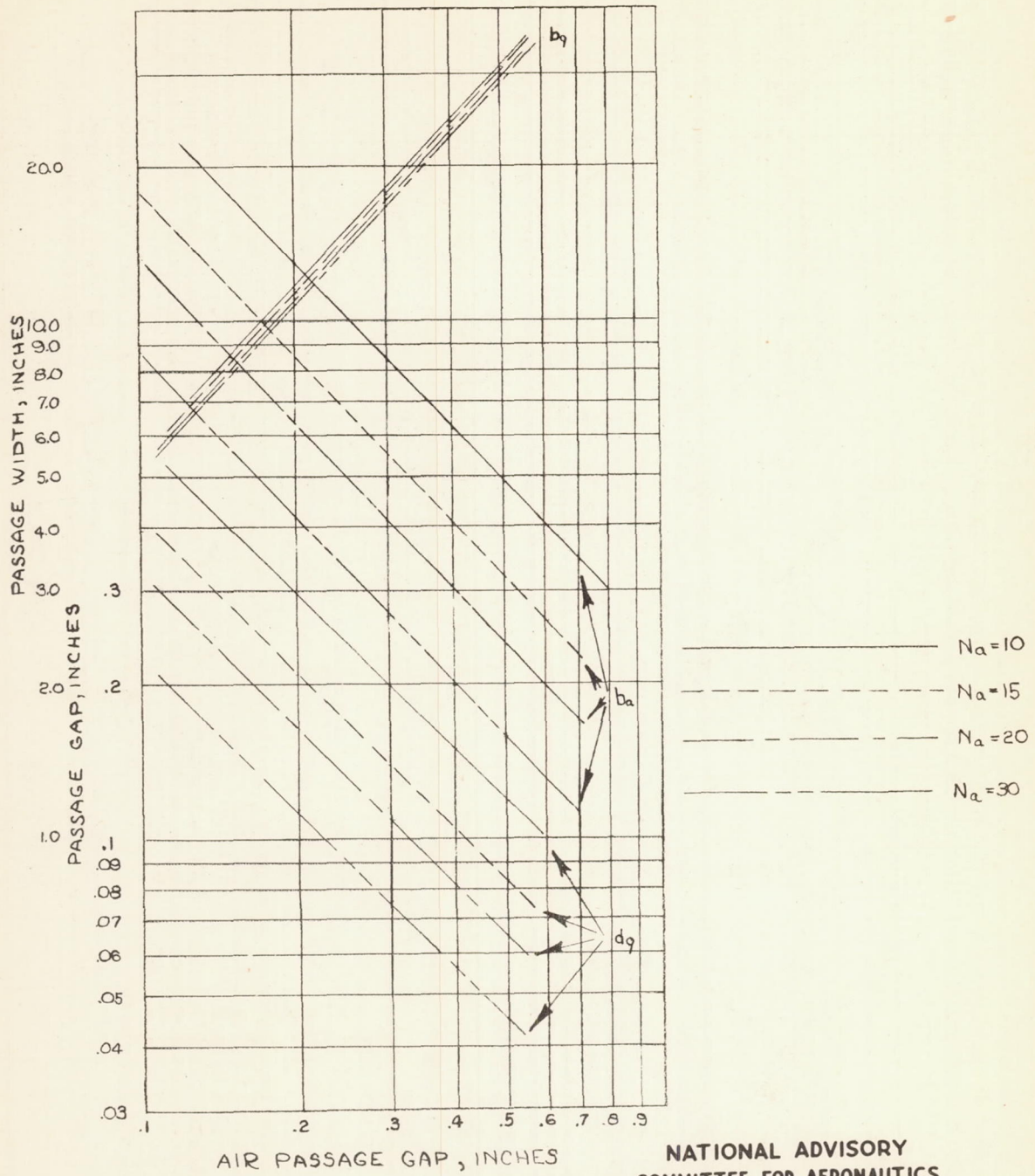
—————  $N_a = 10$                       - - - - -  $N_a = 20$   
 - - - - -  $N_a = 15$                       - · - · -  $N_a = 30$

NATIONAL ADVISORY  
COMMITTEE FOR AERONAUTICS

(b) FINS IN AIR PASSAGES ONLY.

FIGURE 2.-CONTINUED.

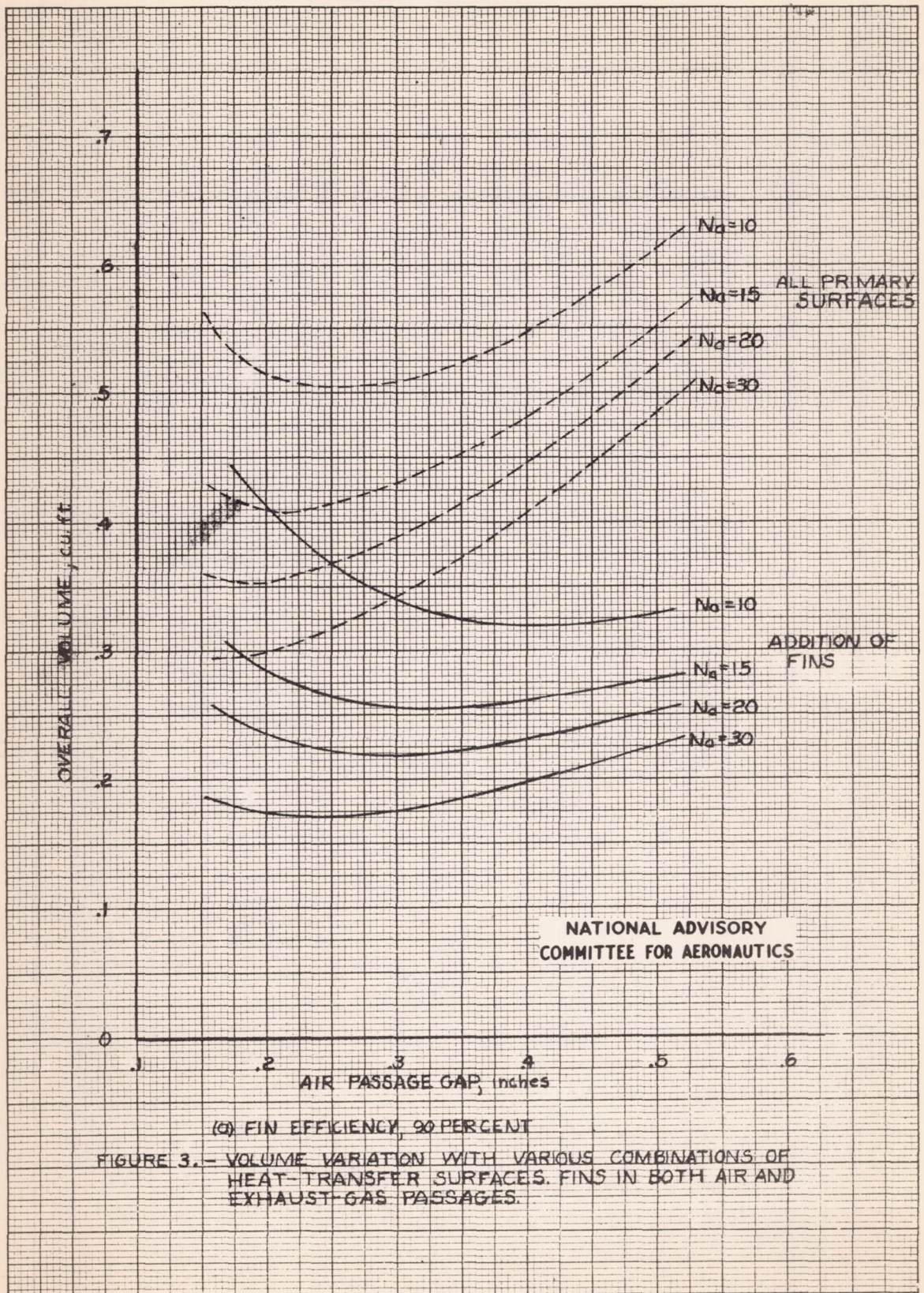
Fig. 2c

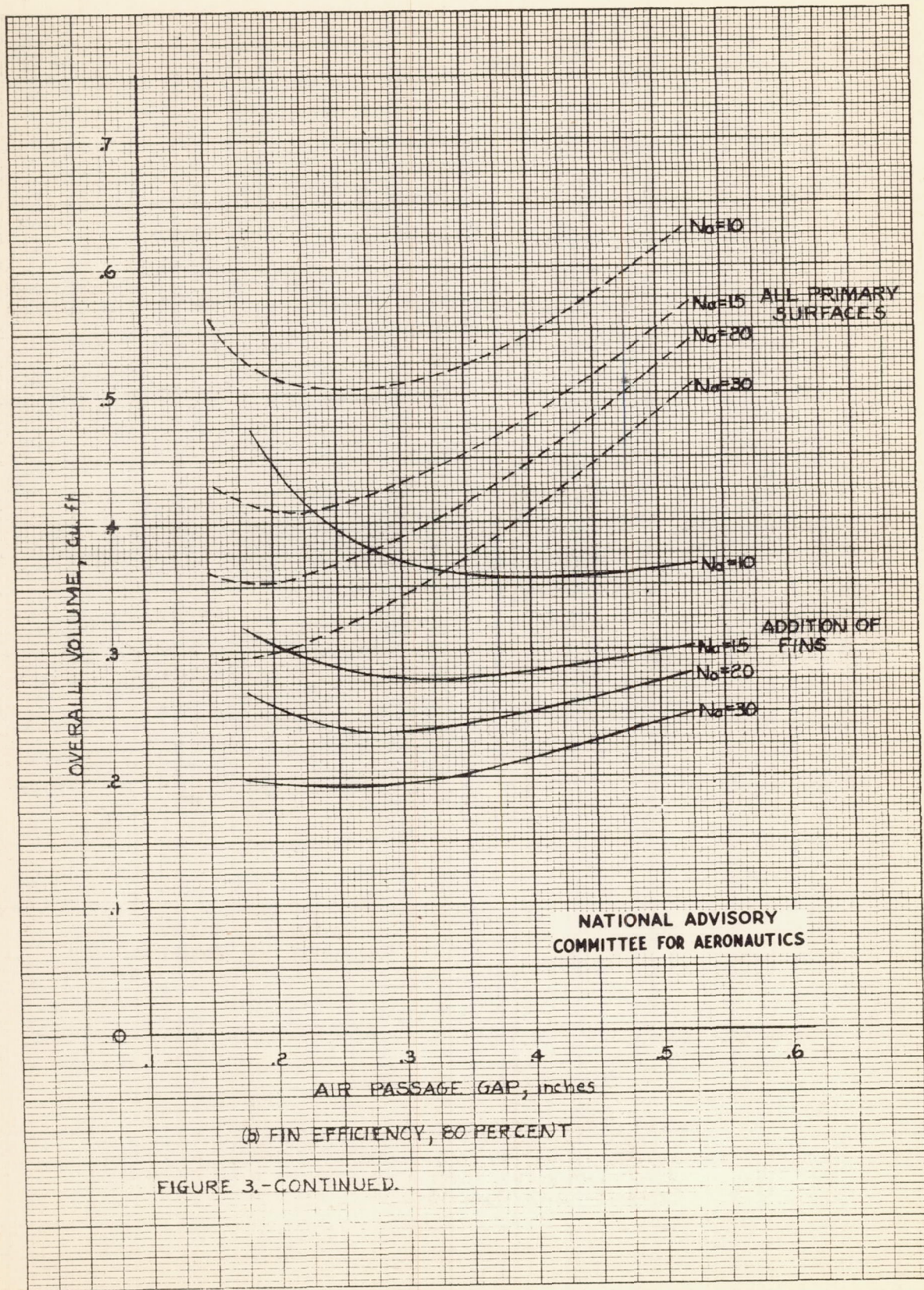


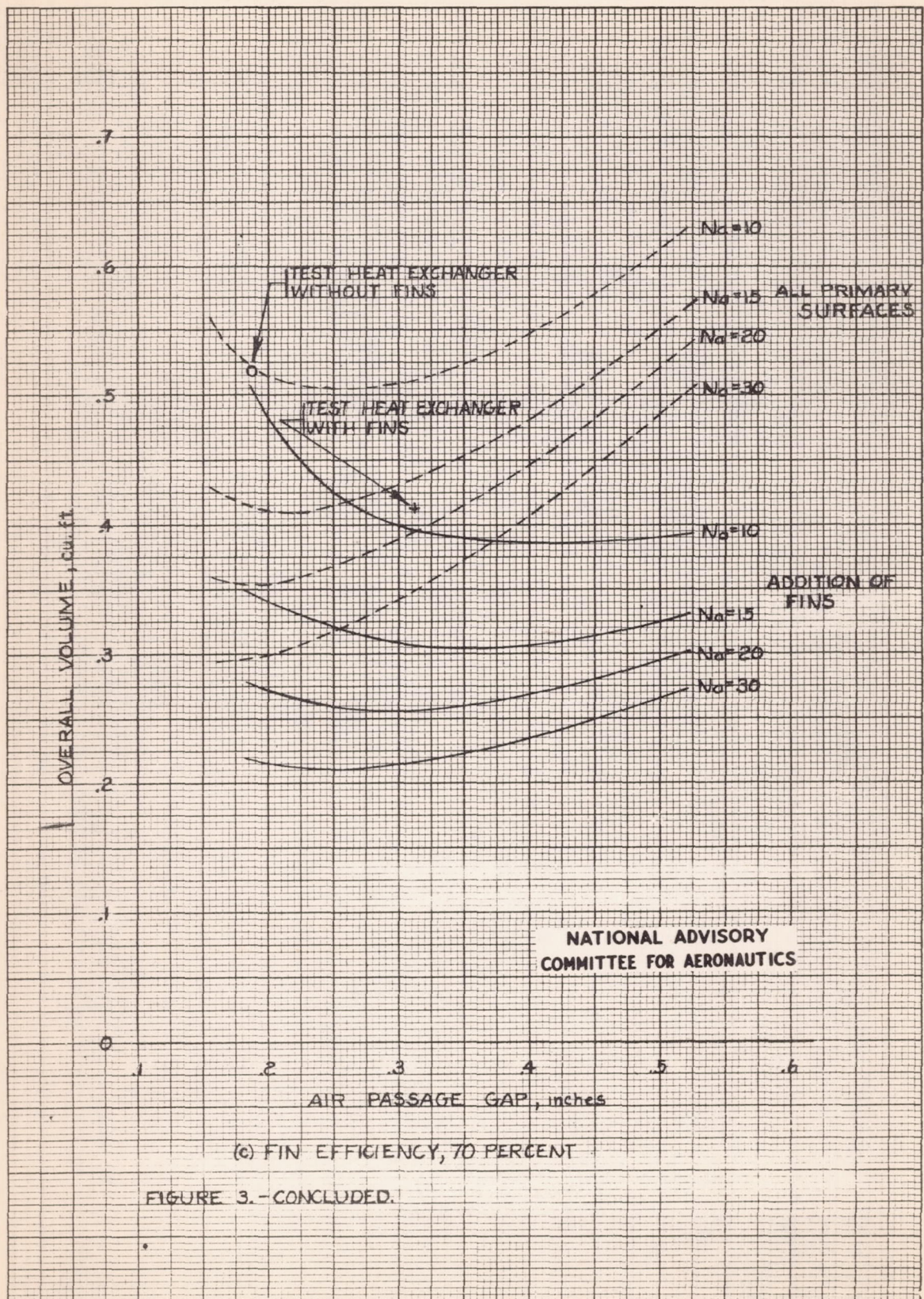
(c) ALL PRIMARY HEAT-TRANSFER SURFACES.

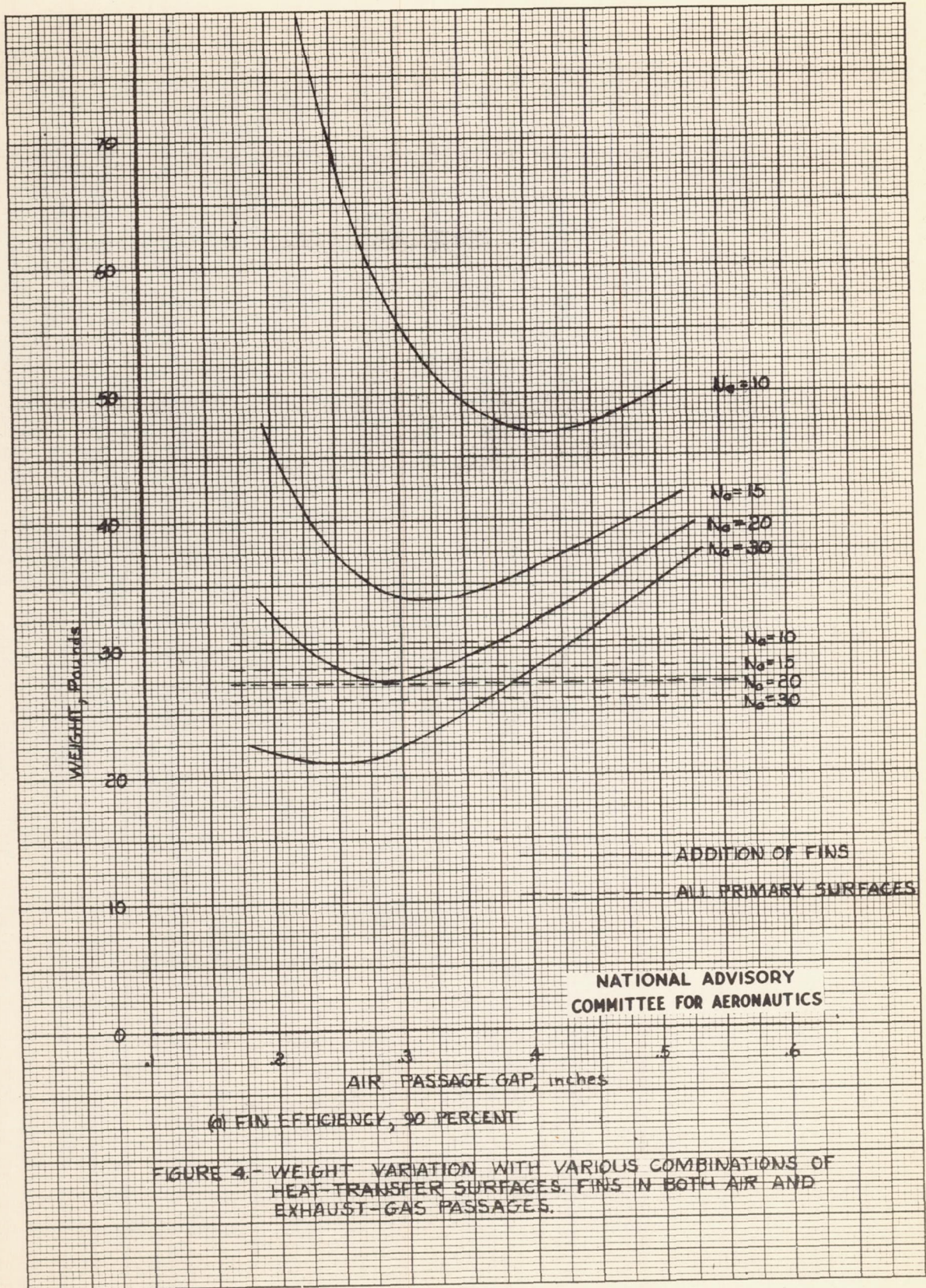
FIGURE 2.-CONCLUDED.

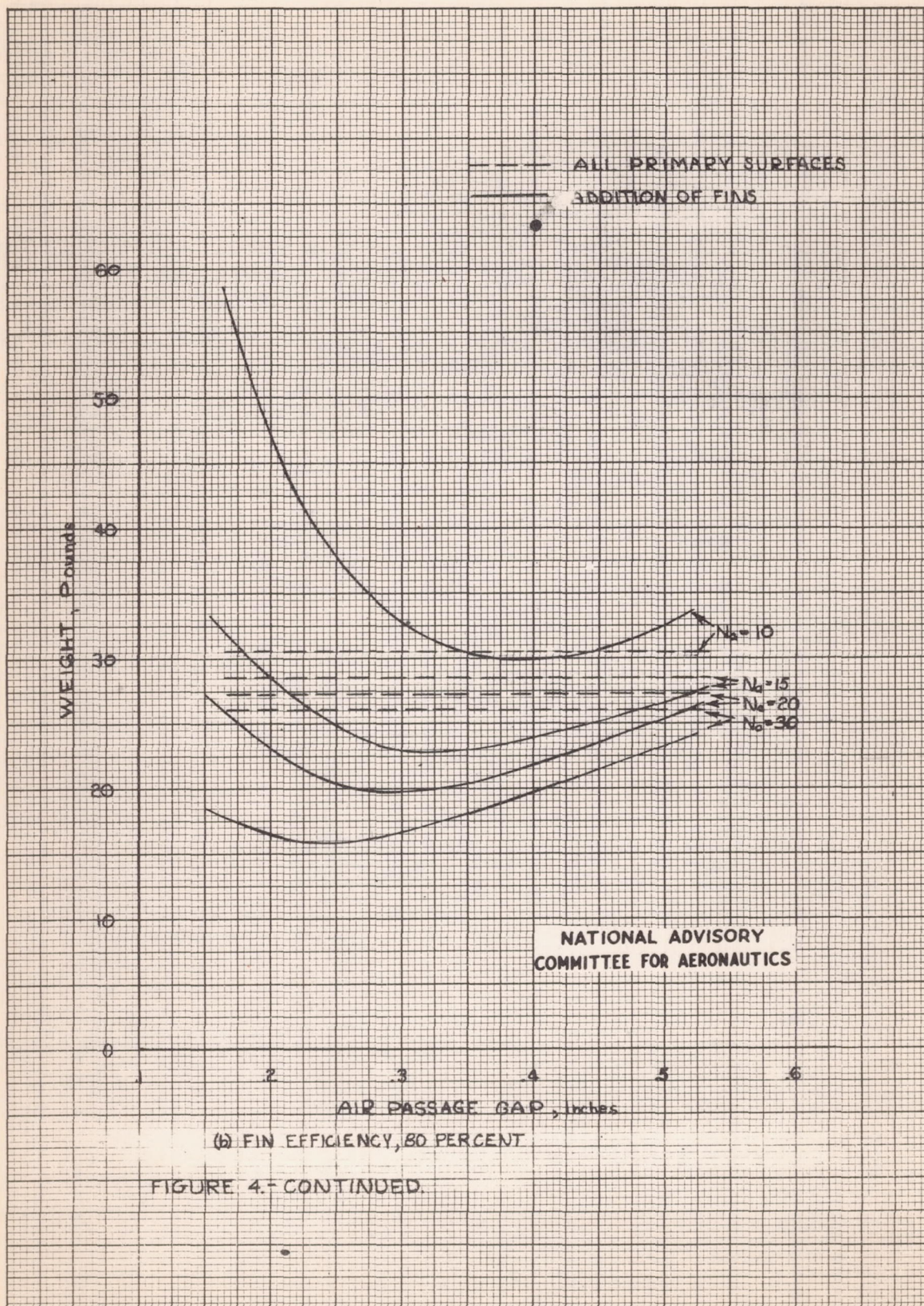


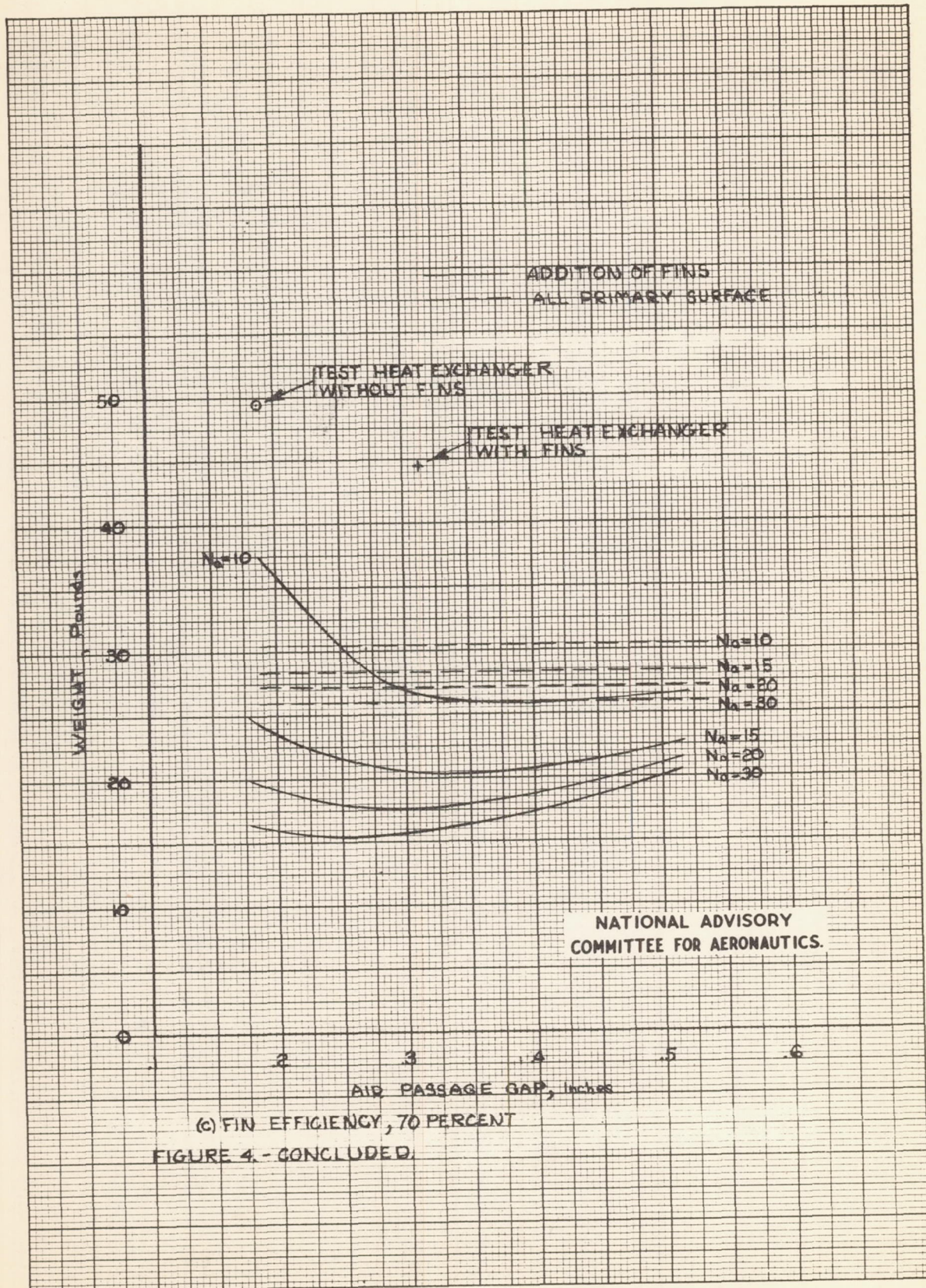












(c) FIN EFFICIENCY, 70 PERCENT

FIGURE 4. - CONCLUDED.

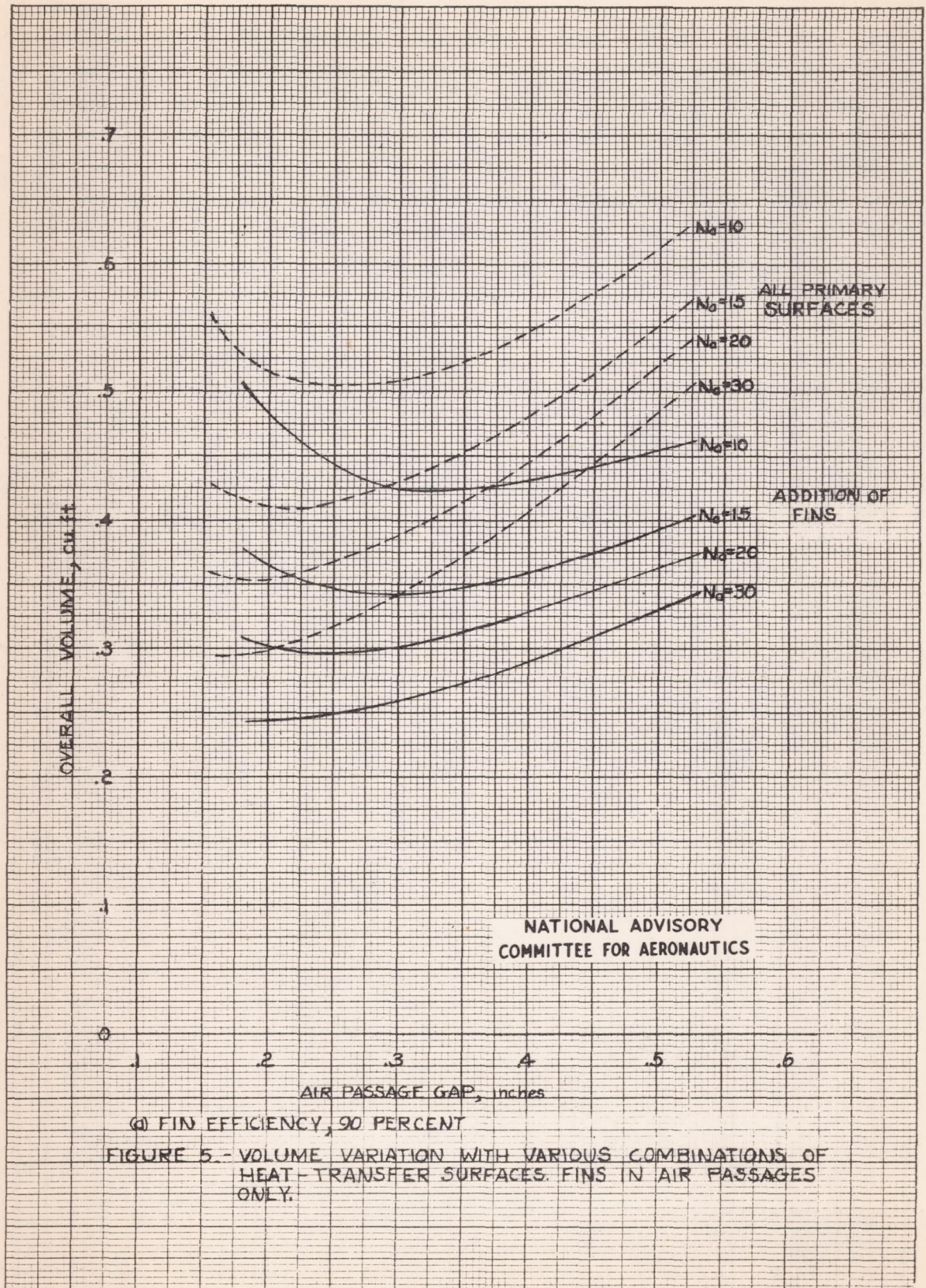
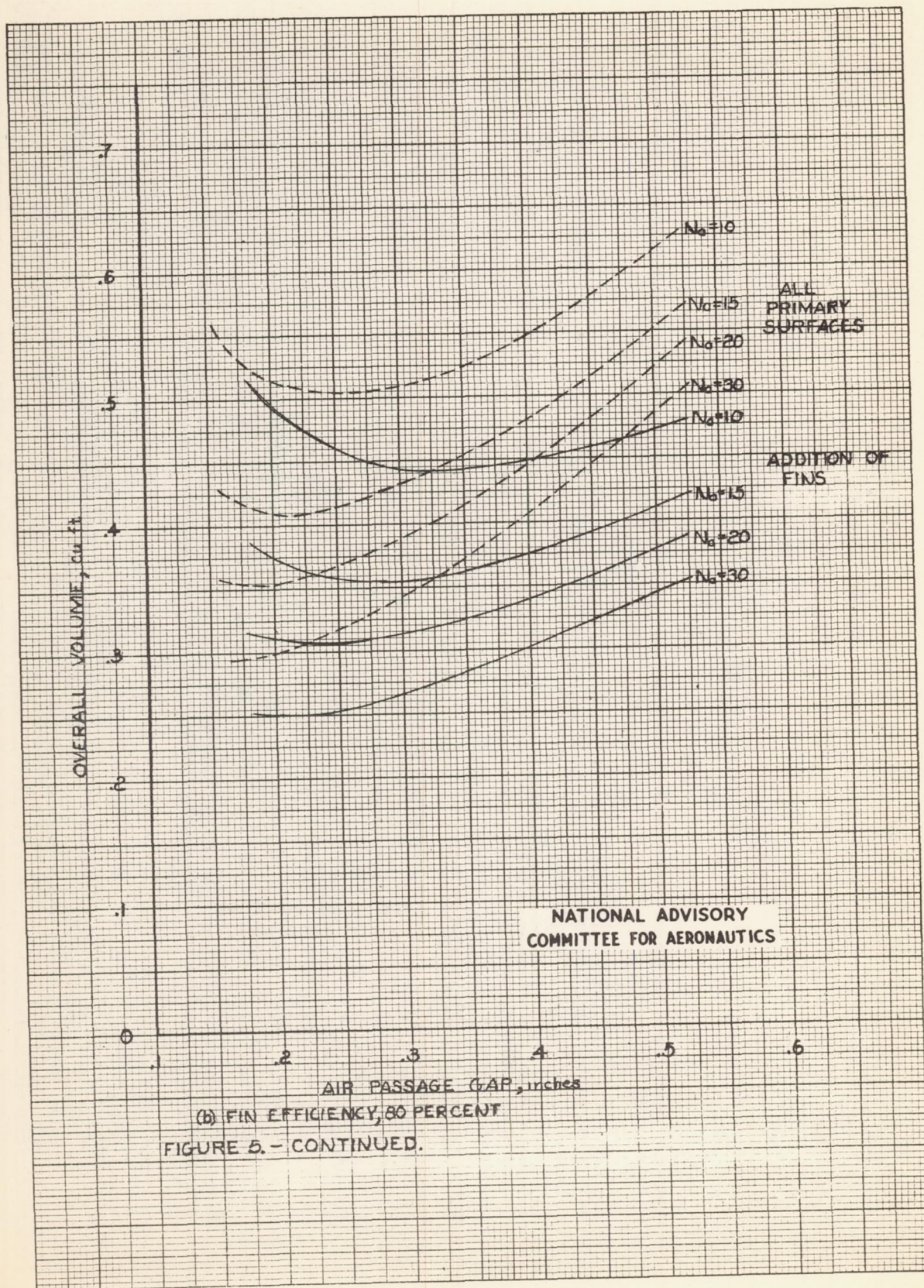
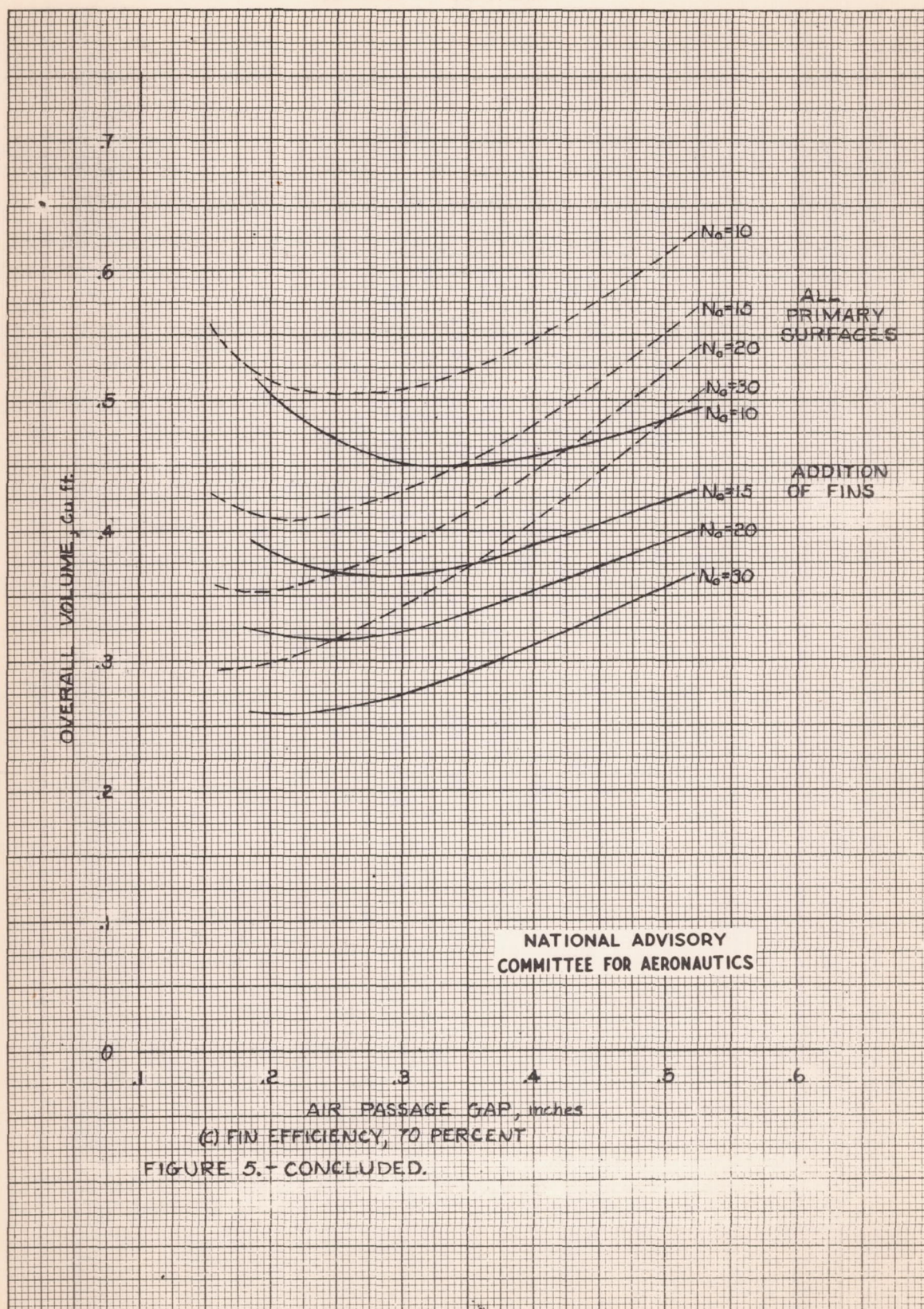
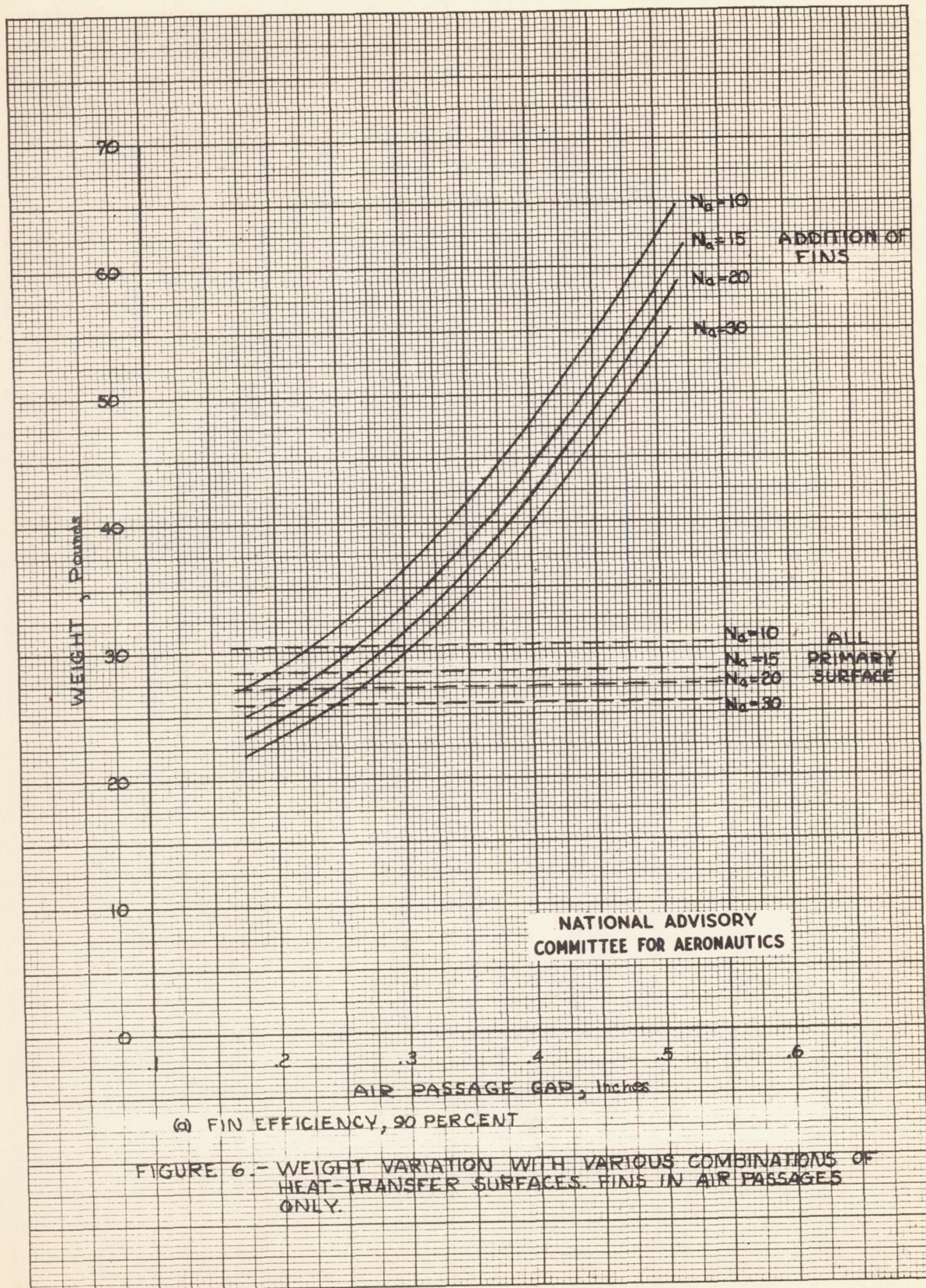


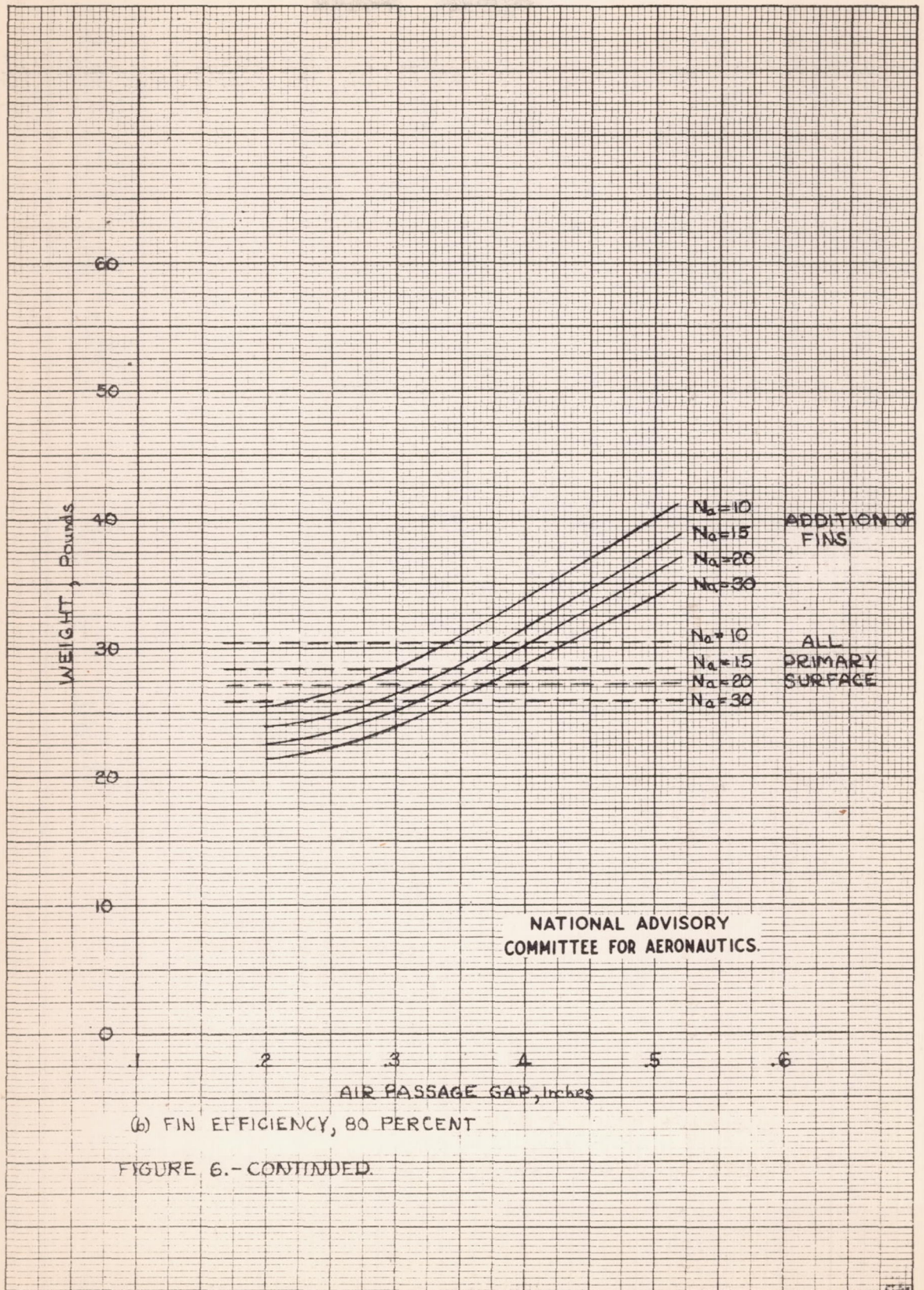
Fig. 5b

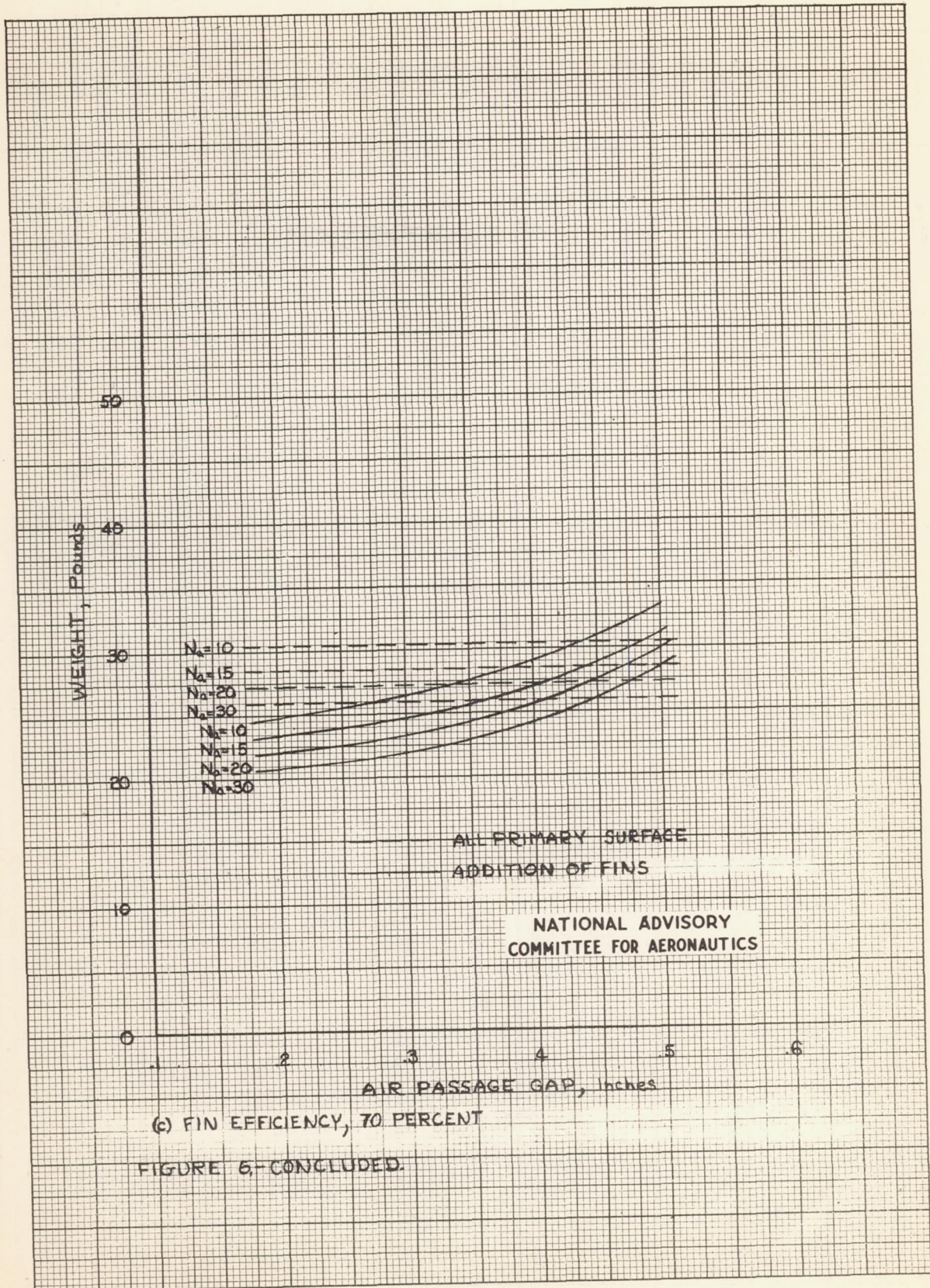




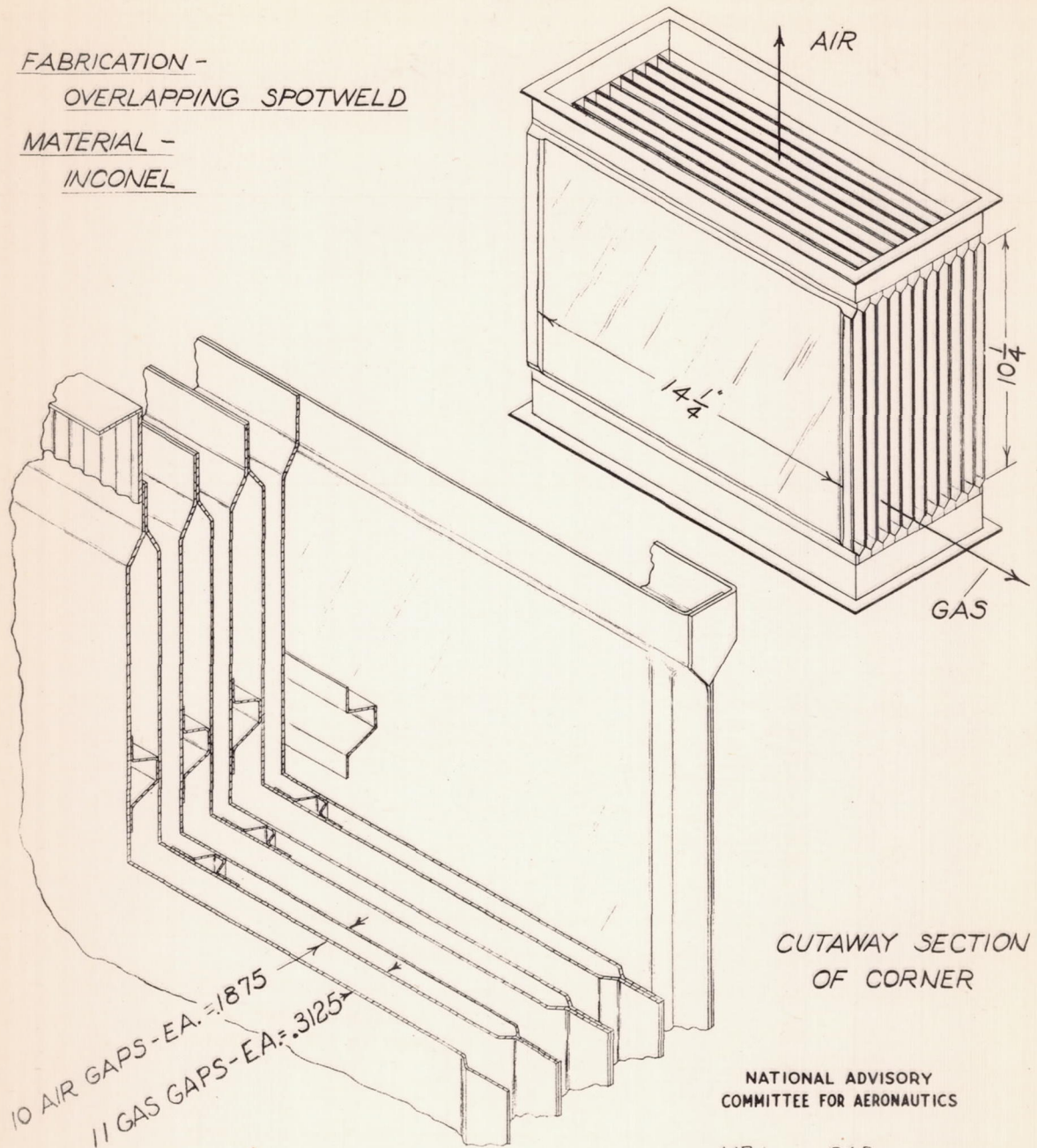








FABRICATION -  
OVERLAPPING SPOTWELD  
MATERIAL -  
INCONEL

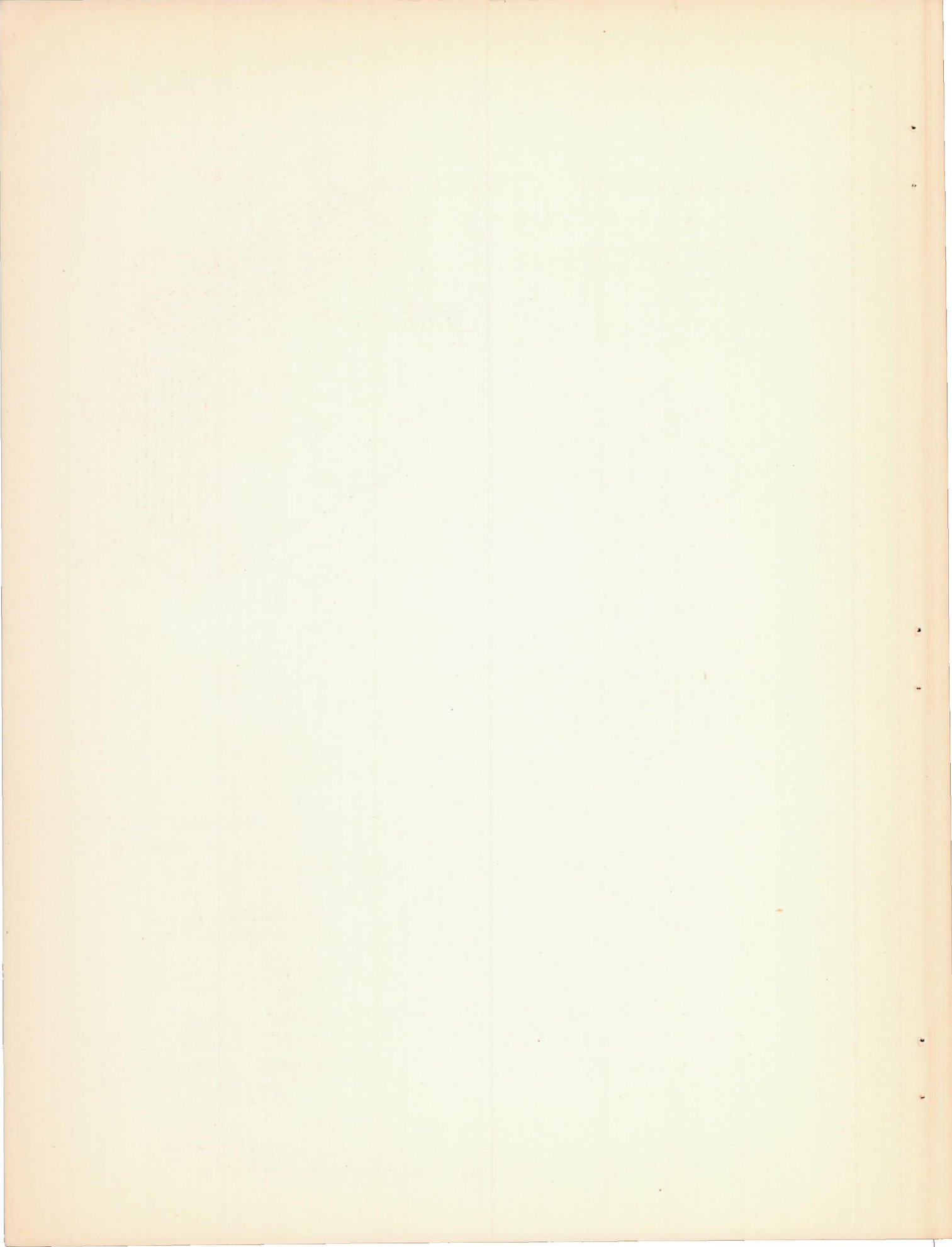


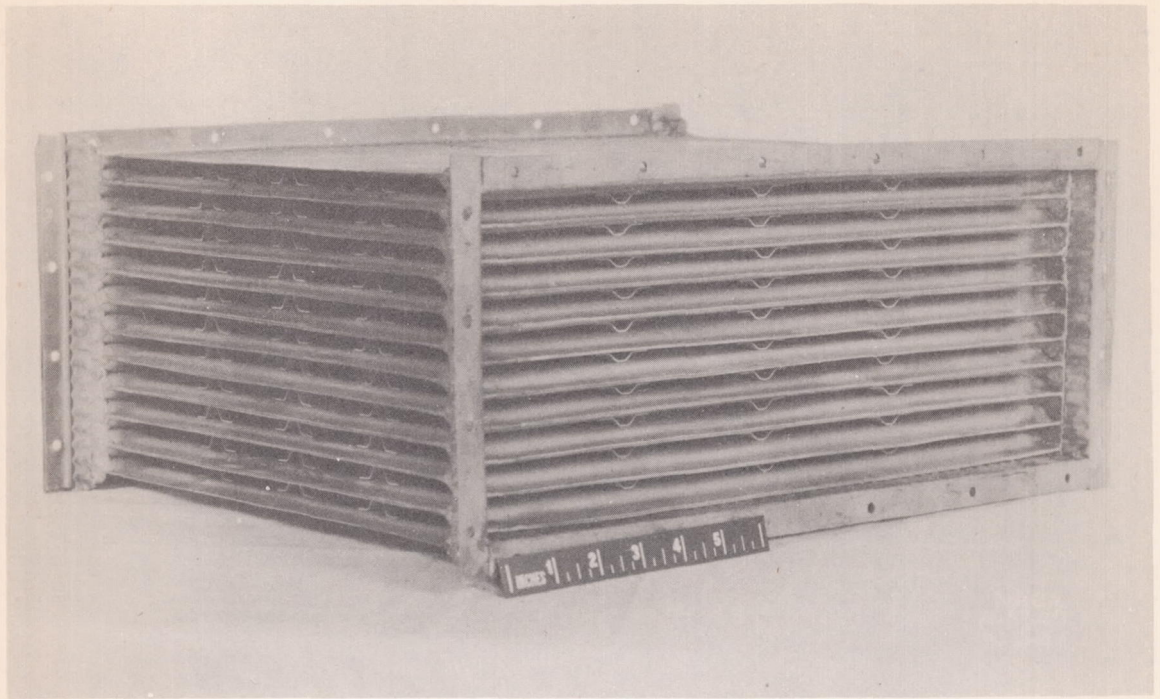
CUTAWAY SECTION  
 OF CORNER

NATIONAL ADVISORY  
 COMMITTEE FOR AERONAUTICS

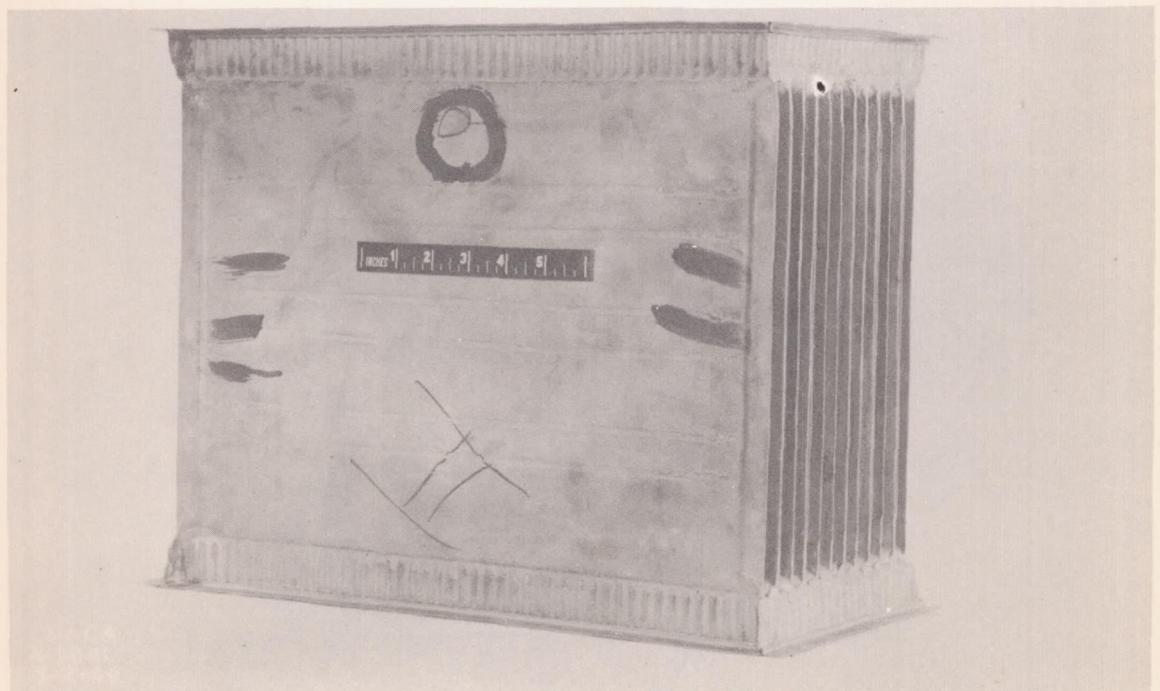
	AIR SIDE	GAS SIDE
PRIMARY HEAT TRANSFER AREA - SQ. FT.	20.3	20.3
MINIMUM FREE AREA - SQ. FT.	0.187	0.249
HYDRAULIC DIAMETER - FT.	0.0285	0.0511
WEIGHT OF CORE	49 1/2 LBS.	

FIGURE 7. DETAILS OF UNFINNED HEAT EXCHANGER CORE



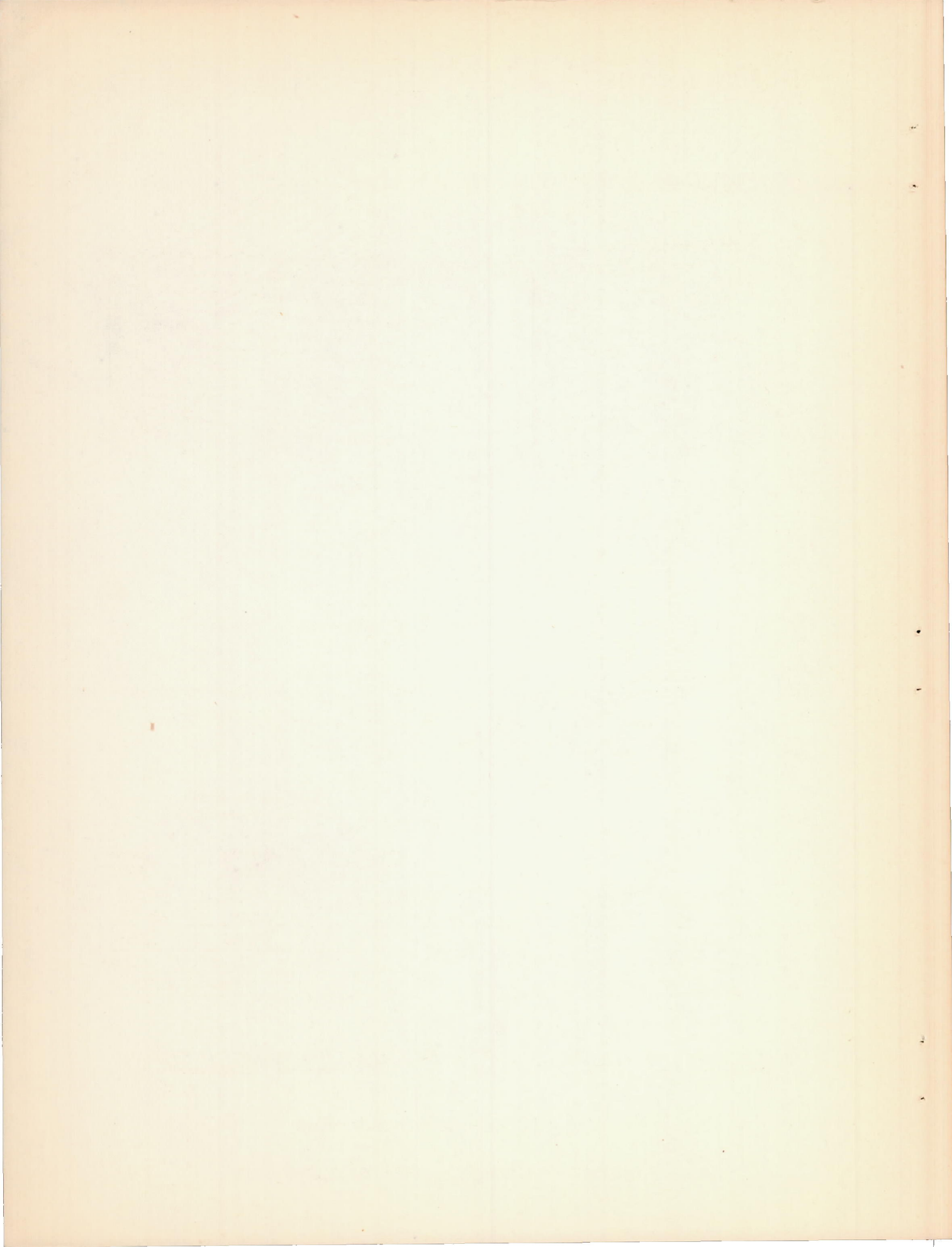


(a) Three-quarter end view.



(b) Three-quarter side view.

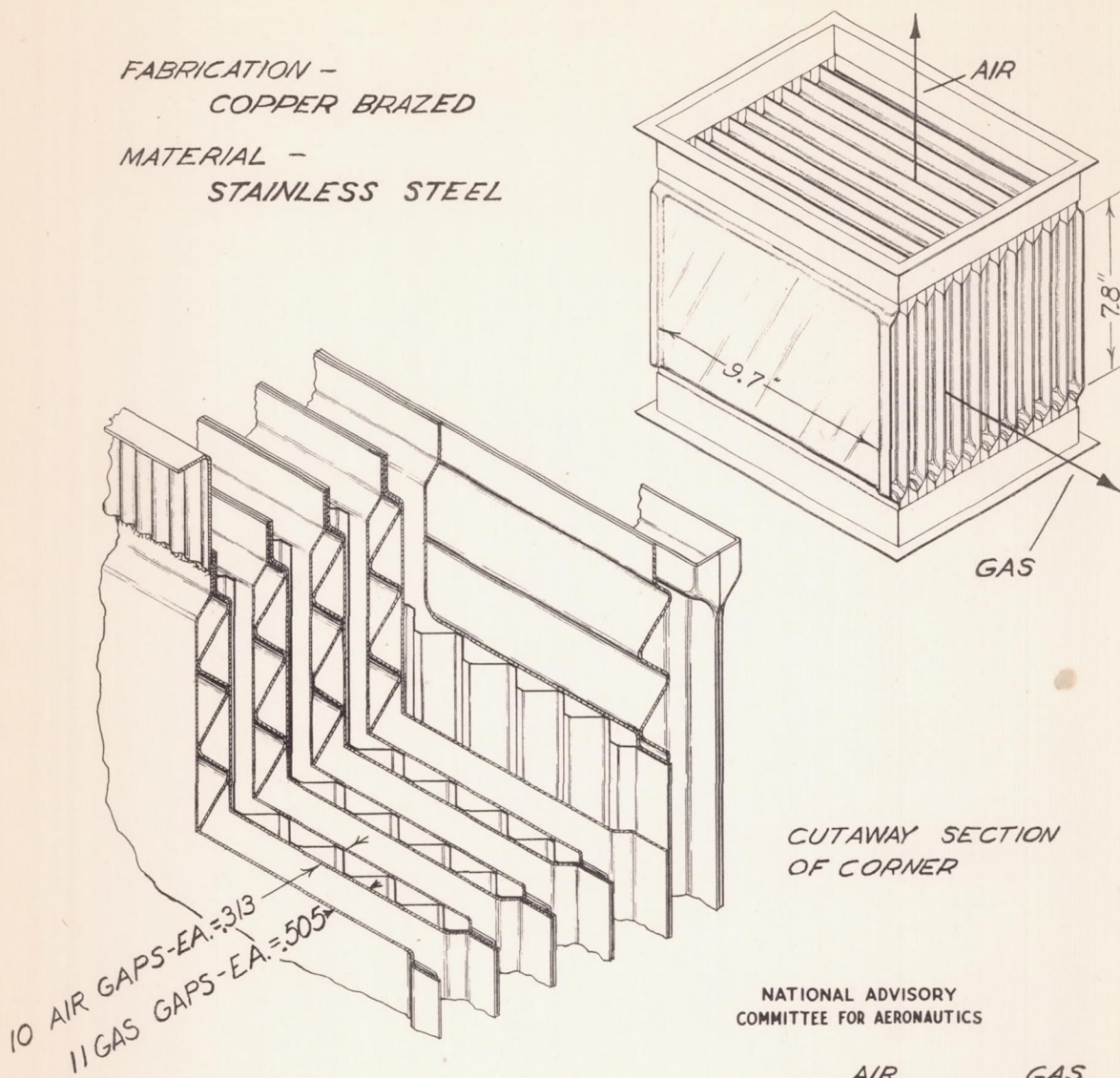
Figure 8.- Unfinned heat-exchanger core.





FABRICATION -  
COPPER BRAZED

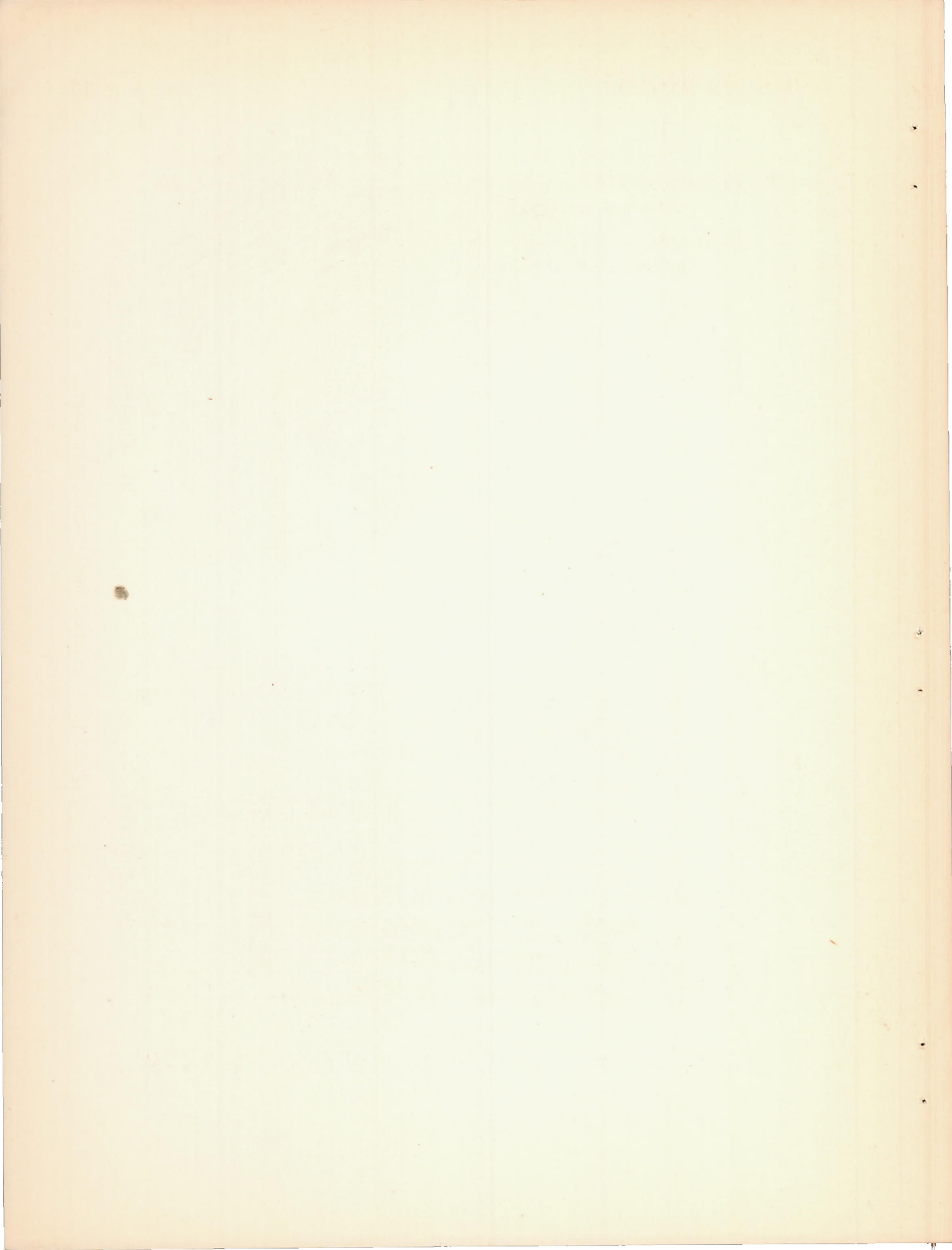
MATERIAL -  
STAINLESS STEEL

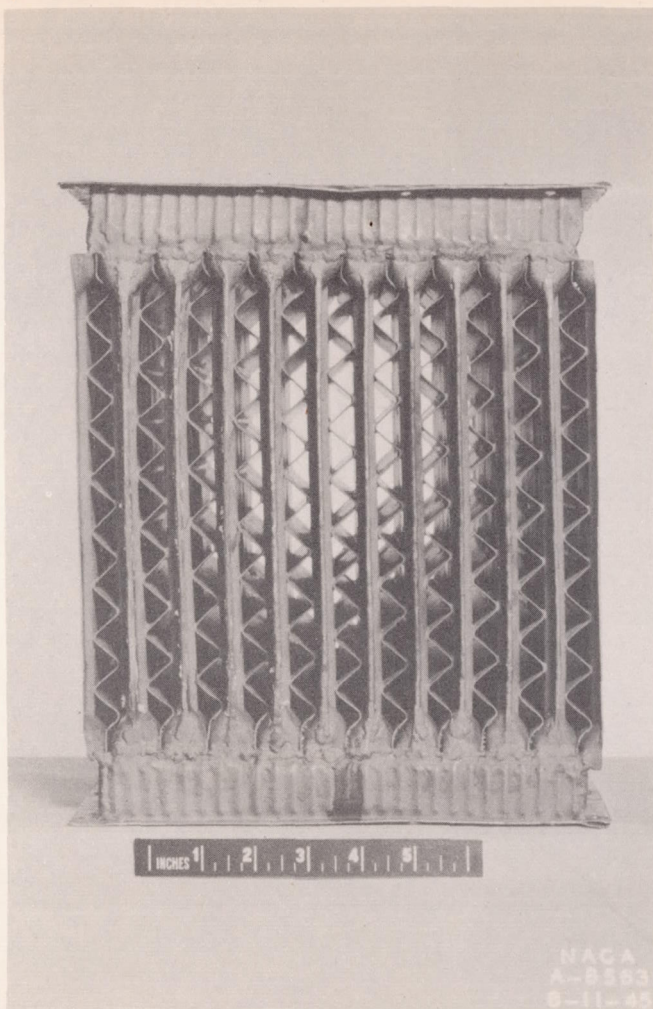


NATIONAL ADVISORY  
COMMITTEE FOR AERONAUTICS

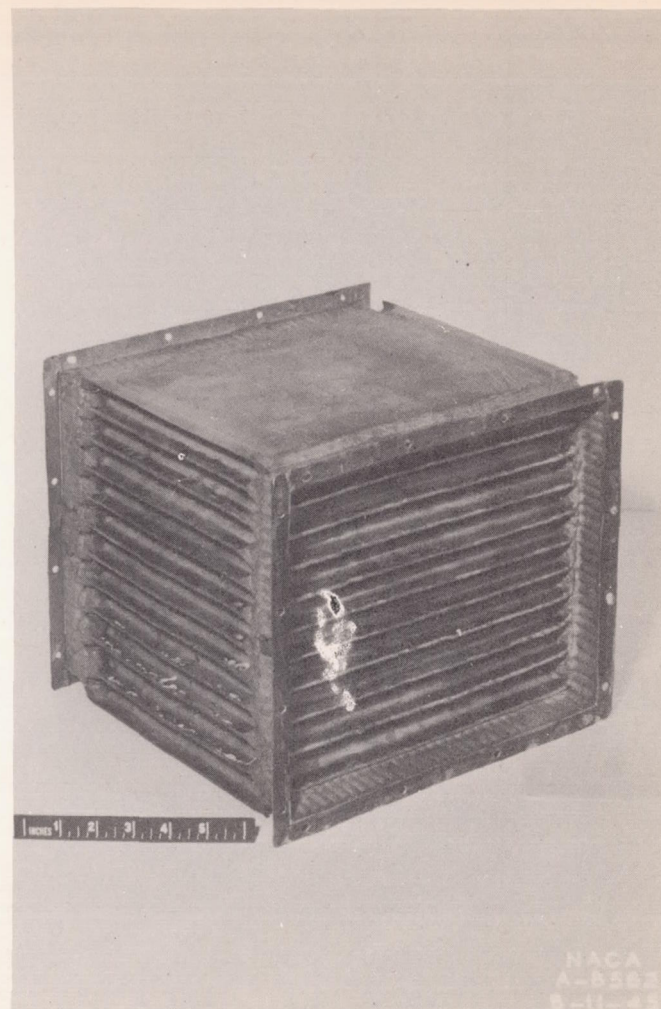
	AIR SIDE	GAS SIDE
PRIMARY HEAT TRANSFER AREA - SQ.FT.	10.55	10.55
FIN HEAT TRANSFER AREA - SQ.FT.	13.05	13.73
MINIMUM FREE AREA - SQ.FT.	.198	.282
HYDRAULIC DIAMETER - FT.	.0216	.0332
WEIGHT OF CORE	44.5 LBS.	

FIGURE 9.-DETAILS OF FINNED HEAT EXCHANGER CORE



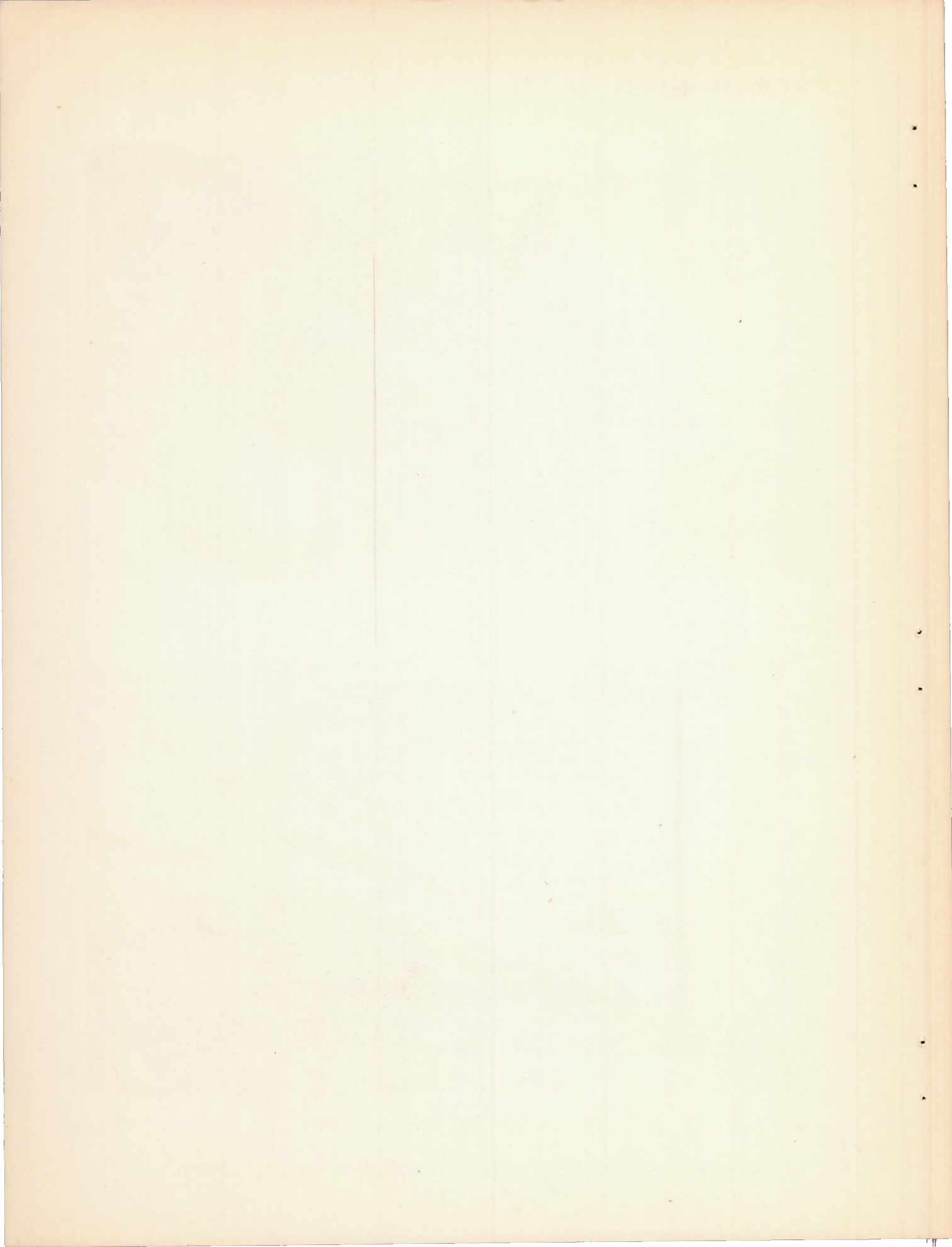


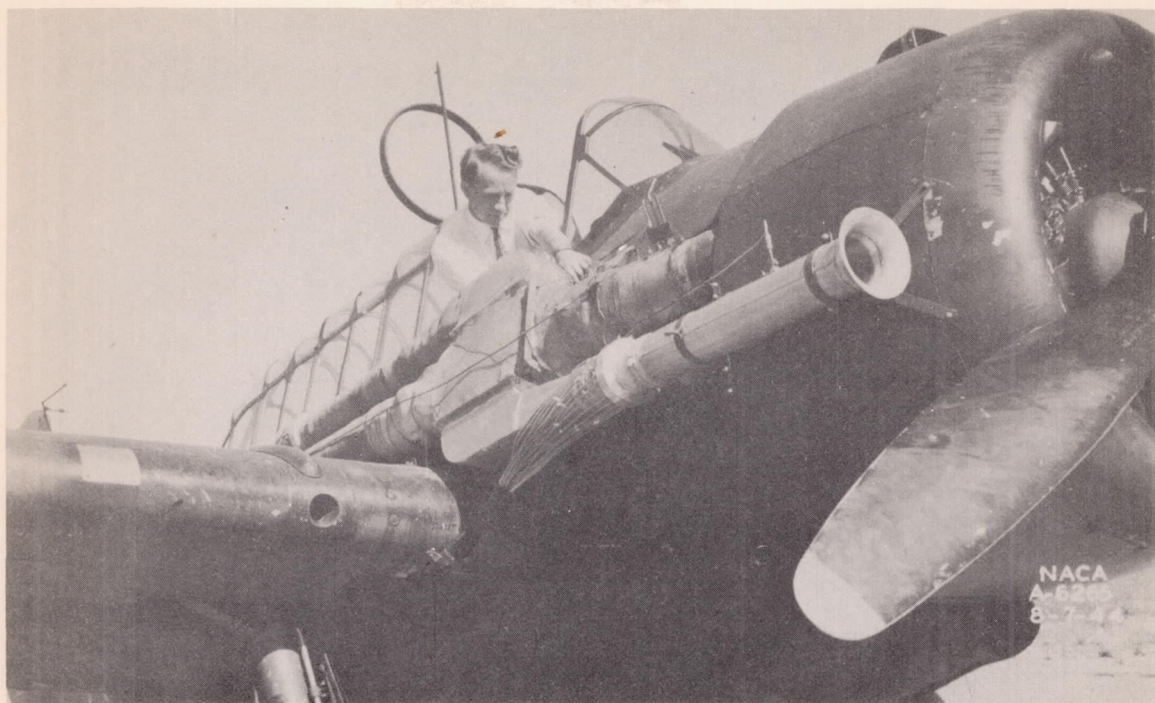
(a) End view.



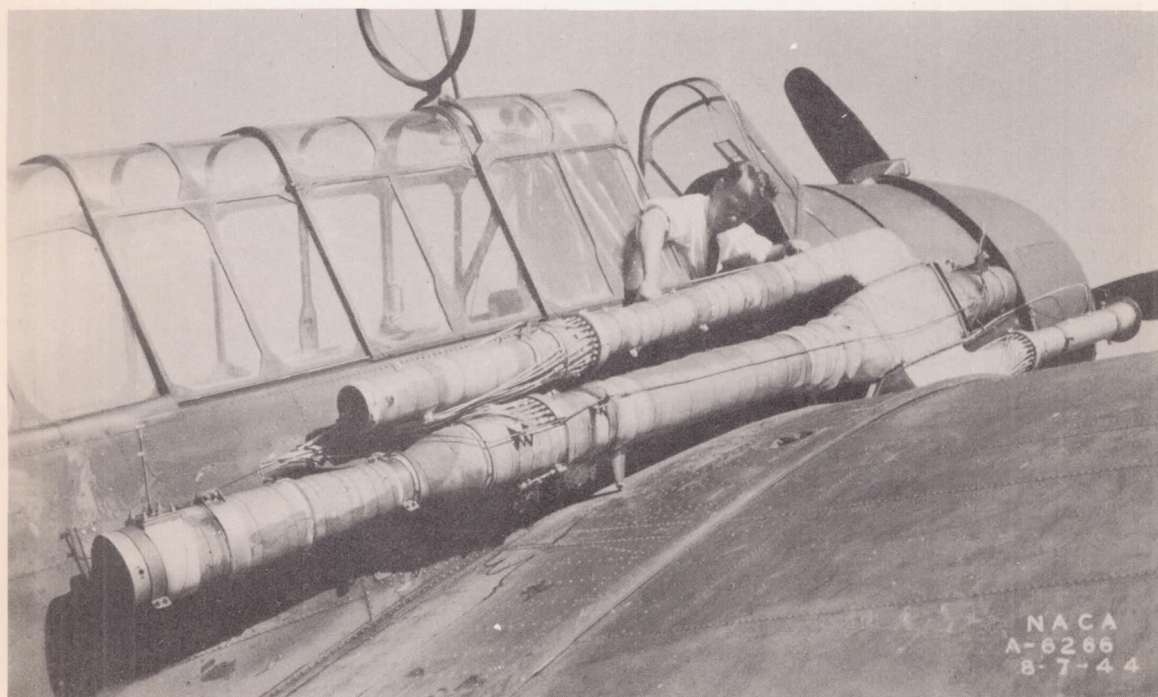
(b) Three-quarter end view.

Figure 10.- Finned heat-exchanger core.



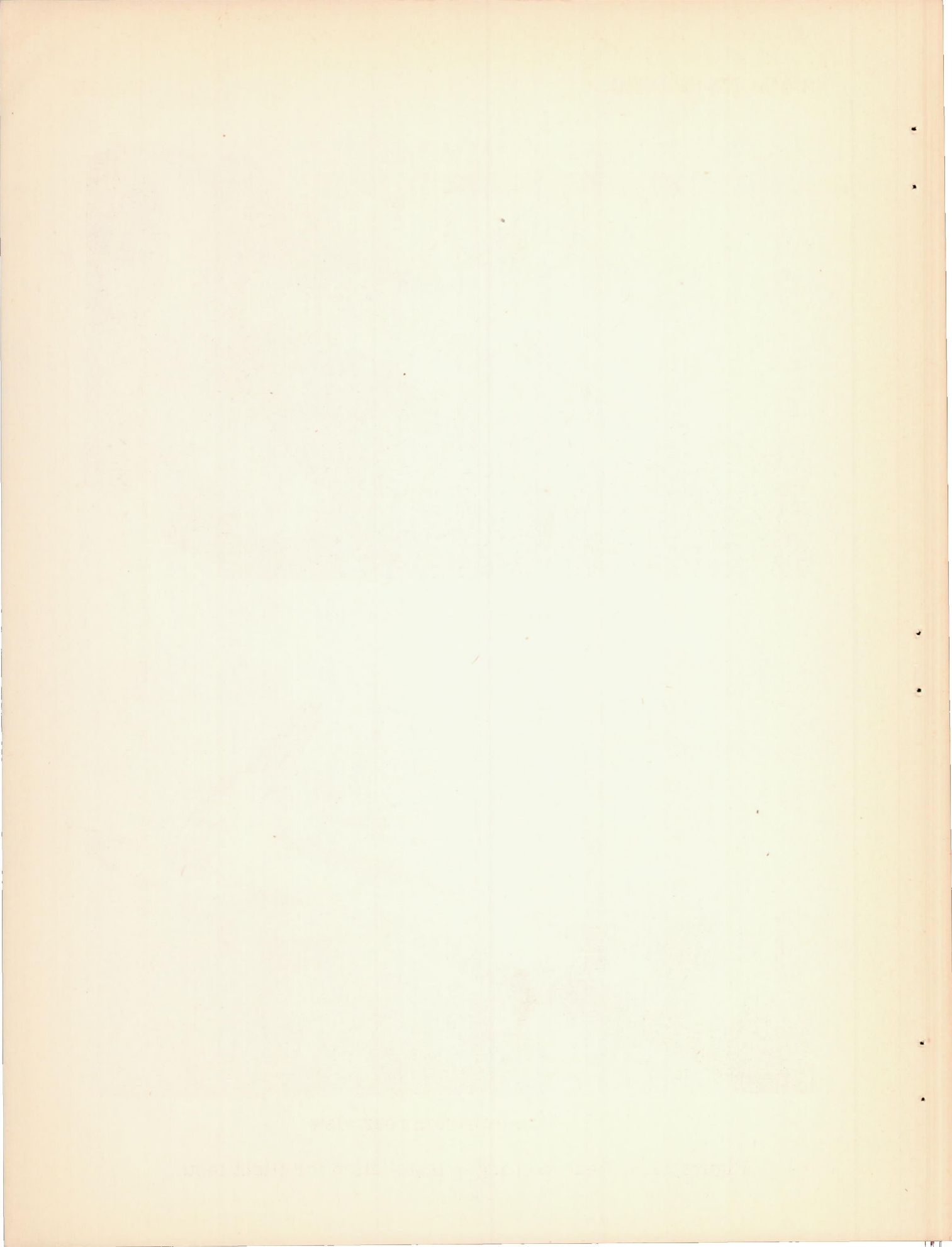


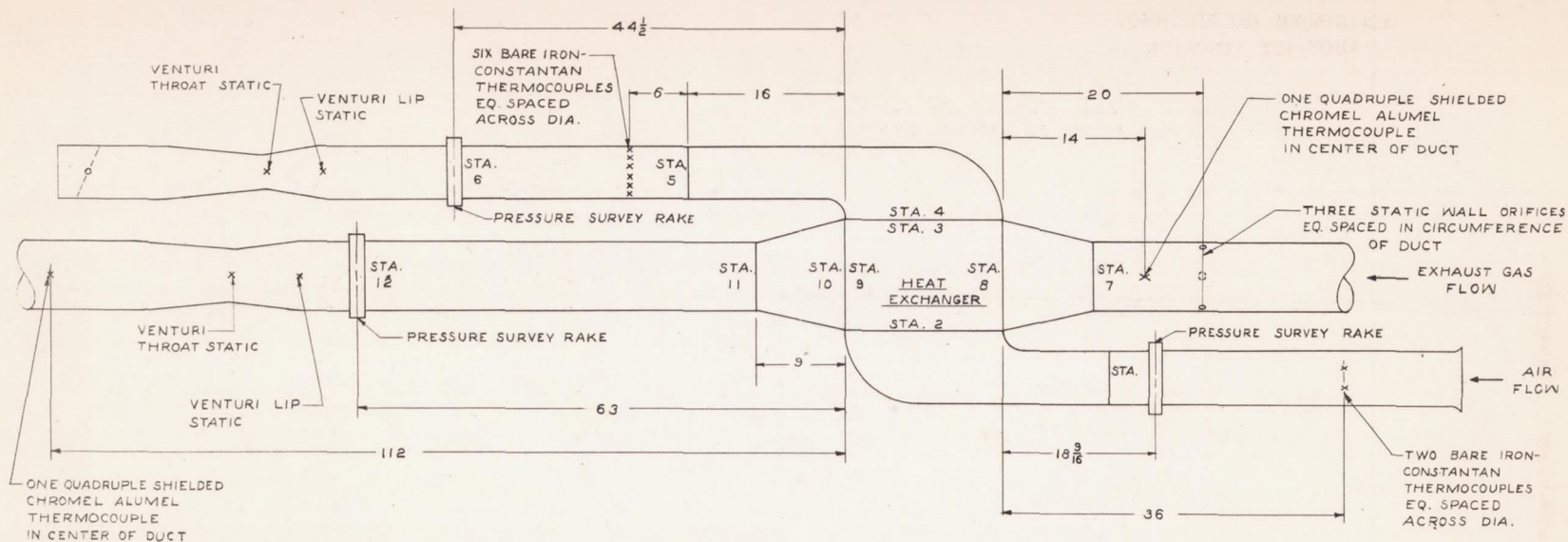
(a) Three-quarter front view.



(b) Three-quarter rear view.

Figure 11.- Heat-exchanger installation for flight tests.



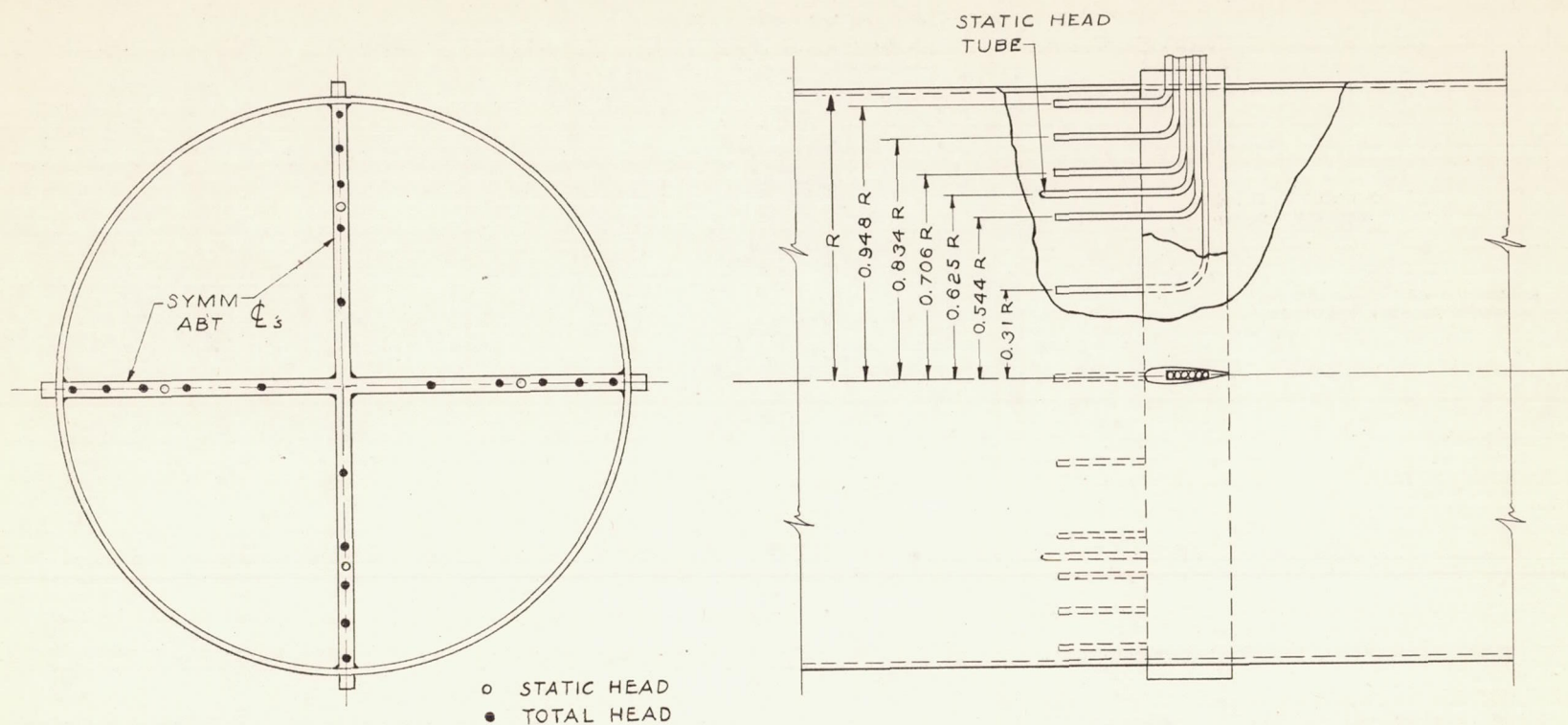


STATION	AREA IN SQ. FT.
1, 5 & 6	0.136
2 & 3	0.167
4	0.646
7, 11 & 12	0.307
8 & 9	0.250
10	0.486

NOTE:  
FOR DETAILS OF PRESSURE  
SURVEY RAKE SEE FIGURE 13

NATIONAL ADVISORY  
COMMITTEE FOR AERONAUTICS

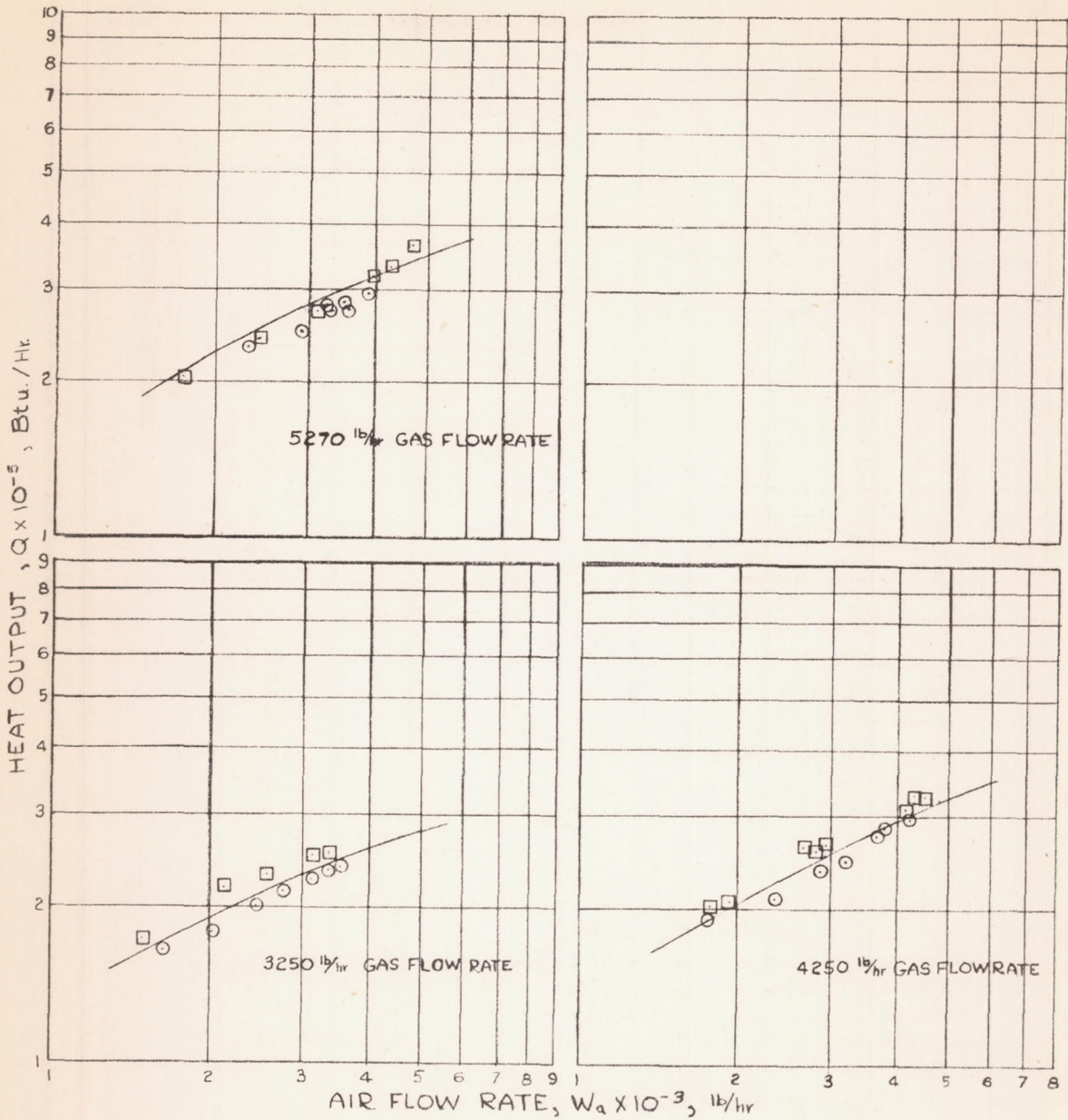
FIGURE 12. LAYOUT OF THE HEAT EXCHANGER AS TESTED IN FLIGHT  
ON THE NORTH AMERICAN 20-47A AIRPLANE



NATIONAL ADVISORY  
COMMITTEE FOR AERONAUTICS

FIGURE 13. LAYOUT OF PRESSURE SURVEY RAKE USED IN FLIGHT TESTS ON  
THE NORTH AMERICAN 20-47A AIRPLANE

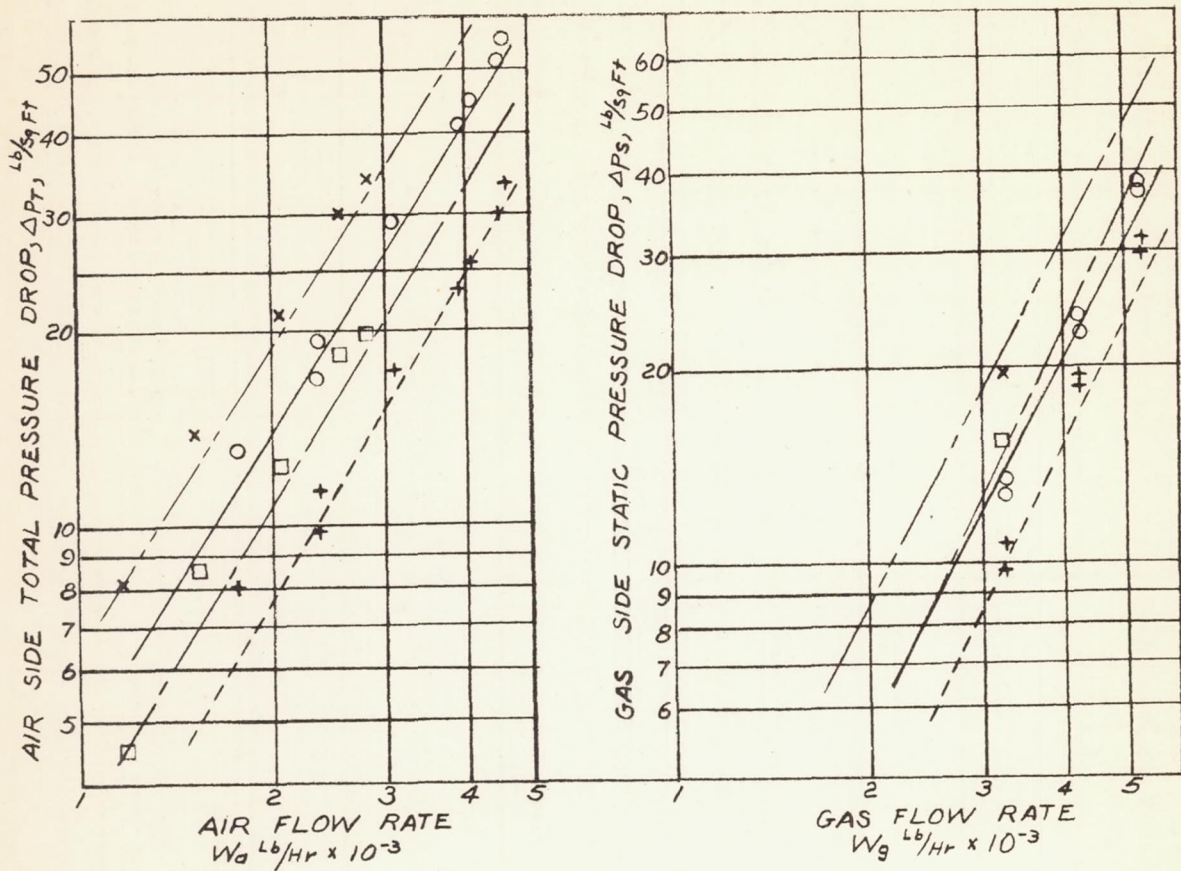




- - TEST POINTS, EXCHANGER WITH FINS
- - TEST POINTS, EXCHANGER WITHOUT FINS
- PREDICTED HEAT OUTPUT, UNFINNED HEAT EXCHANGER

NATIONAL ADVISORY  
COMMITTEE FOR AERONAUTICS

FIGURE 14 - COMPARATIVE THERMAL OUTPUTS OF FINNED AND UNFINNED HEAT EXCHANGERS, DATA REDUCED TO AN INITIAL AIR-EXHAUST GAS TEMPERATURE DIFFERENCE OF 1500°F.



5000 Ft. PRESS. ALT.  $t_{g,in} \cong 1600^{\circ}F, t_{a,in} \cong 60^{\circ}F$

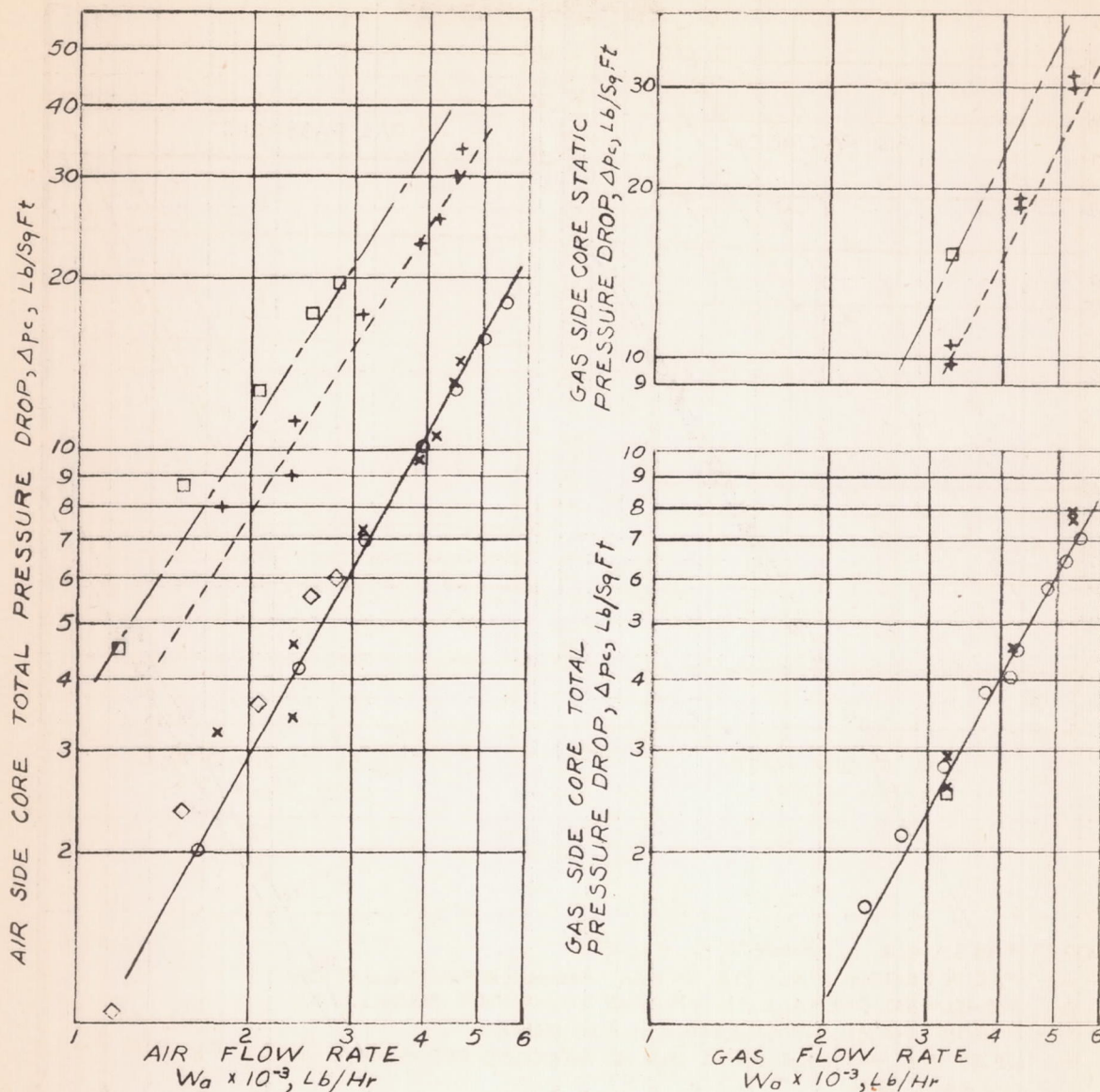
- PREDICTED OVERALL  $\Delta p$  OF HEAT EXCHANGER INSTALLATION
  - o MEASURED OVERALL  $\Delta p$  OF HEAT EXCHANGER INSTALLATION
  - PREDICTED  $\Delta p_c$  HEAT EXCHANGER CORE
  - + HEAT EXCHANGER CORE  $\Delta p_c$  AS REDUCED FROM MEASURED OVERALL  $\Delta p$ .
- }  $(\Delta p_T)_o$  AT  $W_g = 5270 \text{ lb/hr}$

15000 Ft. PRESS. ALT.  $t_{g,in} \cong 1600^{\circ}F, t_{a,in} \cong 60^{\circ}F$

- PREDICTED OVERALL  $\Delta p$  OF HEAT EXCHANGER INSTALLATION
  - x MEASURED OVERALL  $\Delta p$  OF HEAT EXCHANGER INSTALLATION
  - PREDICTED HEAT EXCHANGER CORE  $\Delta p_c$
  - HEAT EXCHANGER CORE  $\Delta p_c$  AS REDUCED FROM MEASURED OVERALL  $\Delta p$
- }  $(\Delta p_T)_o$  AT  $W_g = 3250 \text{ lb/hr}$

NATIONAL ADVISORY  
COMMITTEE FOR AERONAUTICS

FIGURE 15.—NON-ISOTHERMAL PRESSURE DROP OF UNFINNED HEAT-EXCHANGER CORE AS REDUCED FROM MEASURED OVERALL PRESSURE DROP.



NON-ISOTHERMAL PRESSURE DROP

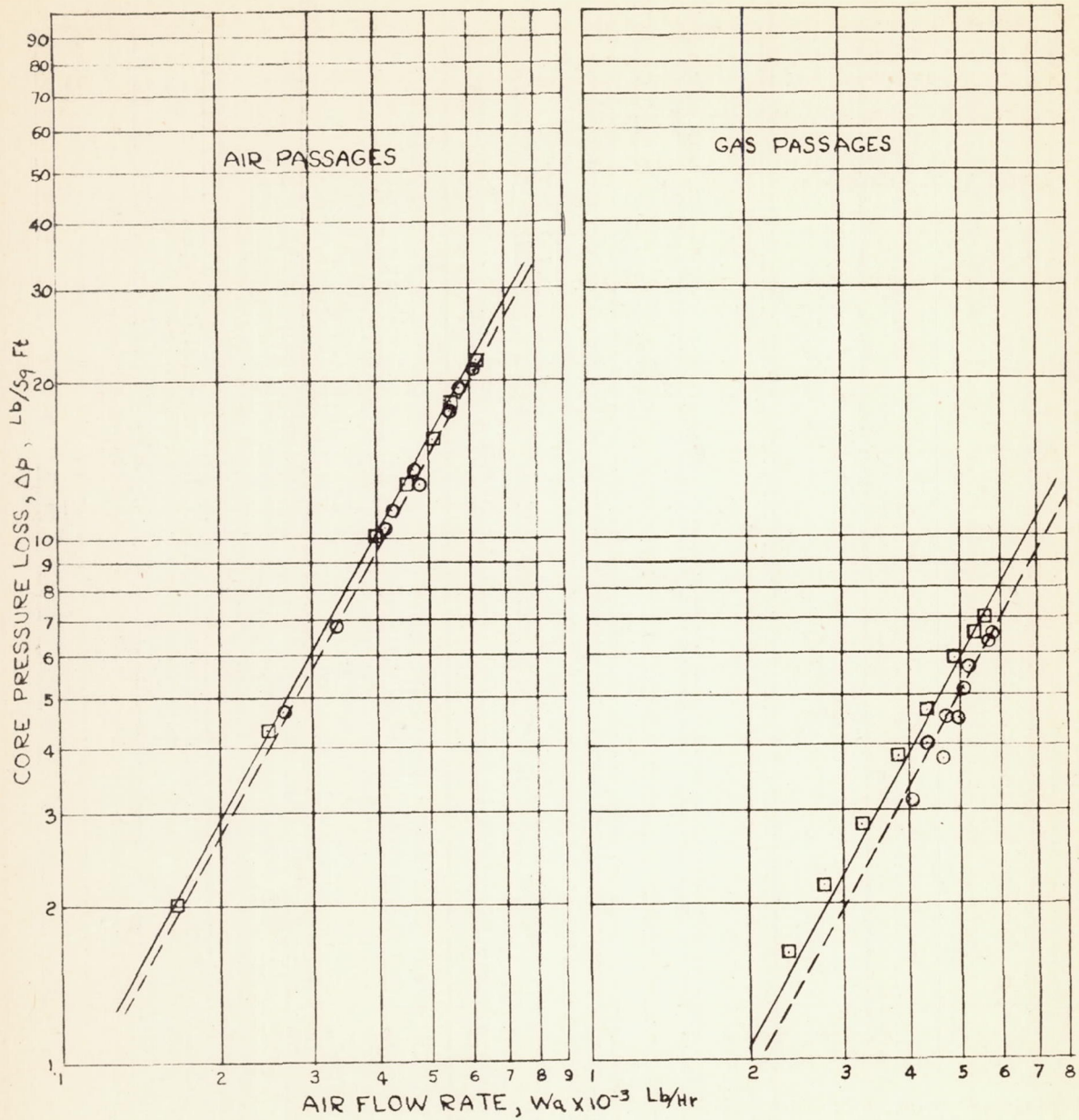
- PREDICTED  $\Delta p_c$  } 5000 FT. PRESSURE ALTITUDE
- + MEASURED  $\Delta p_c$  } ( $\Delta p_c$ )<sub>a</sub> AT  $W_g = 5270$  Lb/Hr
- PREDICTED  $\Delta p_c$  } 15000 FT. PRESSURE ALTITUDE
- MEASURED  $\Delta p_c$  } ( $\Delta p_c$ )<sub>a</sub> AT  $W_g = 3250$  Lb/Hr

ISOTHERMAL PRESSURE DROP AT STANDARD CONDITIONS

- PREDICTED
- MEASURED
- x REDUCED FROM NON-ISOTHERMAL  $\Delta p_c$  AT 5000 FT PRESSURE ALTITUDE
- ◇ REDUCED FROM NON-ISOTHERMAL  $\Delta p_c$  AT 15000 FT PRESSURE ALTITUDE

NATIONAL ADVISORY  
COMMITTEE FOR AERONAUTICS

FIGURE 16.- COMPARISON OF ISOTHERMAL AND REDUCED NON-ISOTHERMAL PRESSURE DROP DATA FOR UNFINED HEAT EXCHANGER AT STANDARD CONDITIONS, 59°F AND 14.7 Lb/Sq in.



- PREDICTED ΔP, HEAT EXCHANGER WITHOUT FINS
- TEST POINTS, HEAT EXCHANGER WITHOUT FINS
- - - PREDICTED ΔP, HEAT EXCHANGER WITH FINS
- TEST POINTS, HEAT EXCHANGER WITH FINS

NATIONAL ADVISORY  
COMMITTEE FOR AERONAUTICS

FIGURE 17.- COMPARATIVE CORE PRESSURE DROPS OF FINNED AND UNFINNED HEAT EXCHANGERS AT STANDARD CONDITIONS, 59°F AND 14.7 Lb/sq in.